Peatland Mid-Infrared Database 1.0.0

Abstract

Systematic collections of peat mid-infrared spectra and other peat properties are scarce, but useful to understand peat chemistry and develop spectral prediction models. The Peatland Mid-Infrared Database ('pmird') stores 3877 mid-infrared spectra of peat, peat-forming vegetation, and dissolved organic matter, together with measurements of other peat properties that were collated from previous studies. Most of the peat samples are from northern bogs, whereas southern or tropical peat and fen peat is underrepresented. The data are supplemented with metadata on sample origin, sample processing, measurements, and quality indicators on whether spectra are baseline corrected or not and on the relative contribution of water vapor, carbon dioxide, and noise to the spectra. The data can be accessed from a MariaDB server and with the R package 'pmird'. The 'pmird' database can be used to analyze peat properties, develop and test spectral prediction models, and develop data and metadata standards.

Henning Teickner[1,2,*]
Svenja Agethen[1]
Sina Berger[3]
Rieke Inga Boelsen[4]
Werner Borken[5]
Luca Bragazza[6]
Tanja Broder[1]
Florentino B. De La Cruz[7]
Andrei-Cosmin Diaconu[8]
Nancy B. Dise[9]
Simon Drollinger[10]
Cristian Estop-Aragonés[1]
Mariusz Gałka[11]
Magalí Martí[12,13]

Stephan Glatzel[14]
Jessica Groß[1]
Lorna Harris[15]
Liam Heffernan[16]
Suzanne B. Hodgkins[17]
Annkathrin Hömberg-Grandjean[1]
Helga Hoppe[1]
Wolfgang Knierzinger[18]
Haojie Liu[19]
Paul J.H. Mathijssen[1,20]
Christopher Mollmann[1]
Wiebke Schuster[21]
Lisa Närtker[1]
David Olefeldt[15]
Verónica Pancotto[22,23]
Nicolas Pelletier[24]
Hendrik Reuter[25]
Bjorn Robroek[26,27]
Bosse Svensson[13]
Julie Talbot[28]
Lauren Thompson[29,30]
Fred Worrall[31]
Zhi-Guo Yu[32]
Klaus-Holger Knorr[1]

[1] Ecohydrology & Biogeochemistry Group, Institute of Landscape Ecology, University of Münster, Germany
[2] Spatiotemporal Modelling Lab, Institute for Geoinformatics, University of Münster, Germany
[3] Pädagogische Hochschule St.Gallen (PHSG), Notkerstrasse 27, 9000 St.Gallen, Switzerland
[4] Albert-Ludwigs-Universität Freiburg, Germany
[5] Soil Ecology, University of Bayreuth, Dr.-Hans-Frisch-Str. 1-3, 95448 Bayreuth, Germany
[6] Agroscope, Field-Crop Systems and Plant Nutrition, Nyon, Switzerland
[7] University of North Florida: Jacksonville, Florida, US
[8] Department of Geology, Babeş-Bolyai University, Kogalniceanu, 1, 400084, Cluj-Napoca, Romania
[9] UK Centre for Ecology & Hydrology Bush Estate, Penicuik, Edinburgh EH26 0QB, United Kingdom
[10] Bioclimatology, University of Göttingen, Göttingen, Germany
[11] University of Lodz, Faculty of Biology and Environmental Protection, Department of Biogeography, Paleoecology and Nature Conservation, Banacha 1/3, 90-237 Łodz, Poland
[12] Department of Biomedical and Clinical Sciences, Linköping University, Linköping, Sweden
[13] Department of Thematic Studies, Environmental Change, Linköping University, 58183 Linköping, Sweden

[14] Department of Geography and Regional Research, Geoecology, Faculty of Earth Sciences, Geography and Astronomy, University of Vienna, Vienna, Austria
[15] Department of Renewable Resources, University of Alberta, Edmonton, AB, T6G 2G7, Canada
[16] Department of Earth Sciences, Earth and Climate Cluster, Vrije Universiteit Amsterdam, Amsterdam, The Netherlands
[17] Department of Microbiology, The Ohio State University, Columbus, OH 43210, USA
[18] Federal Agency for Water Management, Institute for Land and Water Management Research, Petzenkirchen, 3252, Austria
[19] Faculty of Agricultural and Environmental Sciences, University of Rostock, Justus-von-Liebig-Weg 6, 18059 Rostock, Germany
[20] Climate Resilience, Wageningen Environmental Research, Wageningen University & Research, PO Box 47, NL-6700 AA, Wageningen, the Netherland
[21] Stiftung Naturschutz Schleswig-Holstein, Eschenbrook 4, 24113 Molfsee, Germany
[22] Centro Austral de Investigaciones Científicas (CADIC), Consejo Nacional de Investigaciones Científicas y Técnicas (CONICET), Ushuaia, Tierra del Fuego, Argentina
[23] Instituto de Ciencias Polares, Ambiente y Recursos Naturales (ICPA), Universidad Nacional de Tierra del Fuego (UNTDF), Ushuaia, Tierra del Fuego, Argentina
[24] Département de géographie, Université de Montréal, Canada
[25] Department of Ecohydrology and Biogeochemistry, Leibniz Institute of Freshwater Ecology and Inland Fisheries, Berlin, Germany
[26] Department of Ecology, Radboud Institute for Biological and Environmental Sciences, Faculty of Science, Radboud University Nijmegen, 6525 AJ Nijmegen, The Netherlands
[27] School of Biological Sciences, Faculty of Environmental and Life Sciences, University of Southampton, Southampton, SO17 1BJ, UK
[28] Département de Géographie, Université de Montréal, Campus MIL, 1375 Avenue Thérèse Lavoie-Roux, Montréal, Québec, H2V 0B3, Canada
[29] University of Alberta, Department of Renewable Resources, South Academic Building 348D, Edmonton, AB, T6G 2G7
[30] Hatfield Consultants, 1228 Kensington Rd NW Unit 305, Calgary, AB T2N 3P7
[31] Department of Earth Sciences, University of Durham, Durham, DH1 3LE, UK
[32] Ecohydrology Research Group, Dept. Hydrology & Water Resources, Nanjing University of Information Science and Technology, Ningliu Road. 219, 210000 Nanjing
* corresponding author(s): Henning Teickner (henning.teickner@uni-muenster.de)

Background & Summary

Compared to many other soils, peat has a high carbon density[1], and peatlands therefore store more than 500 Gt of carbon[2,3], despite covering only 3% of the land surface[4]. Moreover, because a large part of peat is preserved because of high water table levels that slow down decomposition of the peat organic matter, peatlands can emit comparatively large amounts of carbon when water table levels decrease[5], for example due to land use or climate change[6]. As for other ecosystems, characterizing peatland states and processes and developing process models requires measurements of many peat properties. In addition, a better understanding

of processes requires information on peat molecular structures, for example decomposition processes[7], redox reactions[8,9], or metal accumulation[10].

Mid-infrared spectra (MIRS) are useful for peatland studies because they allow quantification of the relative abundances of many molecular structures. MIRS have been used to estimate the degree of decomposition[11,12,13], the amount of organic matter fractions[14], and — with spectral prediction models — various peat properties, such as element contents, sugar fractions, or pH[14, 15,16]. A database of peat MIRS would facilitate the synthesis of findings across individual studies and the development of robust spectral prediction models, thereby reducing the time and resources required to measure peat properties relevant to characterize peatland states and processes.

Peat samples are underrepresented even in the largest open access soil spectral libraries[16–22]. In addition, many libraries currently do not provide many of the variables relevant for peatland studies. Existing open databases focusing on peatlands[1,23,24] do not contain spectral data. The Peatland Mid-Infrared Database ('pmird' database)[25] addresses this data gap: it contains 3877 mid-infrared spectra of peat, peat-forming vegetation, and dissolved organic matter from peat porewater or peat-covered catchments, as well as data on various peat chemical and physical properties (Tab. 1).

The 'pmird' database is a legacy database that combines data from past studies, many of which are not yet published. The database contains samples from 26 studies worldwide. Most MIRS are transmission Fourier-transform MIRS, but there are also attenuated total reflectance Fourier-transform infrared spectra (ATR-FTIR). In addition to MIRS, 'pmird' contains heterogeneous data on peat physical (bulk densities, radiocarbon ages, ^{210}Pb, ^{226}Ra, ^{137}Cs activities, volumetric water content), chemical (main and trace elemental contents, pH, loss on ignition, electron accepting and donating capacities), and paleoecological (plant macrofossils, testate amoebae) variables, depending on availability for each study.

Due to the legacy nature of the datasets, (meta)data completeness, quality, and validation vary between studies. The 'pmird' database provides as detailed metadata as possible to allow judging which samples and measurements meet specific quality requirements. In addition metadata that summarize the quality of the spectra are provided. Most of the peat samples are from northern bogs, whereas southern and tropical peat and fen peat is underrepresented.

We highlight two applications of the 'pmird' database: first, the database may be used to develop spectral prediction models that predict peat properties from MIRS, for example carbon contents. Second, missing measurements for peat properties in the 'pmird' database can be predicted from already available spectral prediction models to fill data gaps. Since the 'pmird' database contains many samples with spectra, this may allow the creation of a more comprehensive collection of peat samples with estimates for many more peat properties than currently available.

The 'pmird' database is a first attempt to make peat-related MIRS more accessible to researchers, to support the development of community standards for spectral data, and to facilitate research on peatland biogeochemistry. Contributions are welcome and can be proposed via https://github.com/henningte/pmird.

Methods

The 'pmird' database was created by collecting data and metadata of completed and ongoing projects of the biogeochemistry and ecohydrology working group at the Institute for Landscape Ecology (University Münster), collaborating partners at various institutes, and open access data sources.

Collection of suitable datasets

First, a list of potentially available datasets was created. At this stage, the only criterion for inclusion on the list was the availability of MIRS of peat samples (except for data from Liu and Lennartz[26], see below) or related samples (dissolved organic matter, peat-forming vegetation; data from Hodgkins et al.[27] also contain paper and non-peatland vegetation samples that were used in peatland research) and that a data source was known to the first author. From this list, datasets were excluded when no permission for publication could be obtained. Datasets were included if they met the following conditions: either the data are published under an open access license compatible with the CC-BY 4.0 license, or the authors or responsible parties allowed publication of their data under the CC-BY 4.0 license. Data authors or responsible parties were contacted via email describing the project's scope and aims, were asked for permission to use the data and to provide access to data and relevant metadata. Key characteristics of the datasets included in the 'pmird' database and references to original data sources are presented in Tab. 1 and an overview on the spatial distribution of samples is given in Fig. 1.

Table 1: Summary of the datasets included into the pmird database. "ID" is a unique identifier for each dataset in pmird. "No. MIRS" is the number of samples for which a MIRS is available. "Peat properties" are peat properties which were measured at least for one sample in the dataset. "MIRS mode" describes the MIRS measurement mode (ATR-FTIR: Attenuated total reflectance-Fourier transformed infrared, Absorbance-FTIR: Absorbance-Fourier transformed infrared). "Reference" are original references for the dataset.

ID	No. Samples	No. MIRS	Peat properties	MIRS mode	References
1	397	397	Klason_lignin_content, holocellulose_content, age_14C, trace elements	ATR-FTIR	[27,28]
2	138	45	loss_on_ignition, age_14C, lab_code_14C, trace elements	Absorbance-FTIR	[29,30]
3	469	289	N, C, S, P, d13C, d15N, bulk_density, age_14C, lab_code_14C, trace elements	Absorbance-FTIR	[31–33]
4	216	212	N, C, d13C, d15N, mass, volume, bulk_density, loss_on_ignition, pH, trace elements	Absorbance-FTIR	[34,35]
5	78	78	N, C, S, P, d13C, d15N, bulk_density, pH, age_14C, lab_code_14C, porosity, trace elements	Absorbance-FTIR	[36]
6	36	36	N, C, S, P, pH, water_content, trace elements	Absorbance-FTIR	[37]
7	785	227	N, C, S, P, bulk_density, loss_on_ignition, age_14C, lab_code_14C, activity_210Pb, mass_210Pb, CaCO3, water_content, macrofossils, trace elements	Absorbance-FTIR	[38–40]
8	146	96	N, C, d13C, d15N, mass, volume, bulk_density, pH, water_content, trace elements	Absorbance-FTIR	
9	59	59	N, C, O, H, S, P, d13C, d15N, electron_accepting_capacity, electron_donating_capacity, Fe2, Fe3, trace elements	-	[41,42]
10	791	108	N, C, bulk_density, loss_on_ignition, age_14C, macrofossils, trace elements	-	[43,44]
11	79	79	N, C, d13C, d15N, trace elements	Absorbance-FTIR	[45]
12	557	191	N, C, S, P, d13C, d15N, mass, volume, bulk_density, age_14C, water_content, macrofossils, trace elements	Absorbance-FTIR	[46,47]
13	320	309	N, C, S, bulk_density, activity_210Pb, mass_210Pb, background_activity_reached_210Pb, activity_137Cs, year_137Cs, activity_226Ra, trace elements	-	
14	98	97	N, C, S, P, d13C, d15N, Fe2, Fe3, trace elements	Absorbance-FTIR	[48]
15	102	90	N, C, S, P, d13C, d15N, mass, volume, bulk_density, age_14C, trace elements	Absorbance-FTIR	[49]
16	298	96	N, C, S, P, mass, volume, bulk_density, activity_210Pb, mass_210Pb, activity_137Cs, year_137Cs, activity_226Ra, water_content, trace elements	ATR-FTIR, Absorbance-FTIR	[50,51]
17	114	114	trace elements	Absorbance-FTIR	[52]
18	1102	123	N, C, S, P, d13C, d15N, bulk_density, loss_on_ignition, age_14C, lab_code_14C, macrofossils, trace elements	Absorbance-FTIR	[53]
19	523	82	N, C, S, P, d13C, d15N, age_14C, lab_code_14C, macrofossils, trace elements	Absorbance-FTIR	[54]
20	634	124	N, C, S, P, d13C, d15N, bulk_density, loss_on_ignition, age_14C, lab_code_14C, macrofossils, trace elements	Absorbance-FTIR	[55]
21	138	48	bulk_density, trace elements	Absorbance-FTIR	[56,57]
22	106	85	N, C, O, H, S, trace elements	Absorbance-FTIR	[58,59]
23	1955	380	N, C, d13C, d15N, bulk_density, loss_on_ignition, age_14C, lab_code_14C, macrofossils, trace elements	Absorbance-FTIR	
24	54	54	N, C, trace elements	Absorbance-FTIR	[60–62]
25	380	0	bulk_density, loss_on_ignition, hydraulic_conductivity, porosity, macroporosity, trace elements	-	[26]
26	1641	446	N, C, S, bulk_density, activity_210Pb, mass_210Pb, trace elements	Absorbance-FTIR	[63,64]

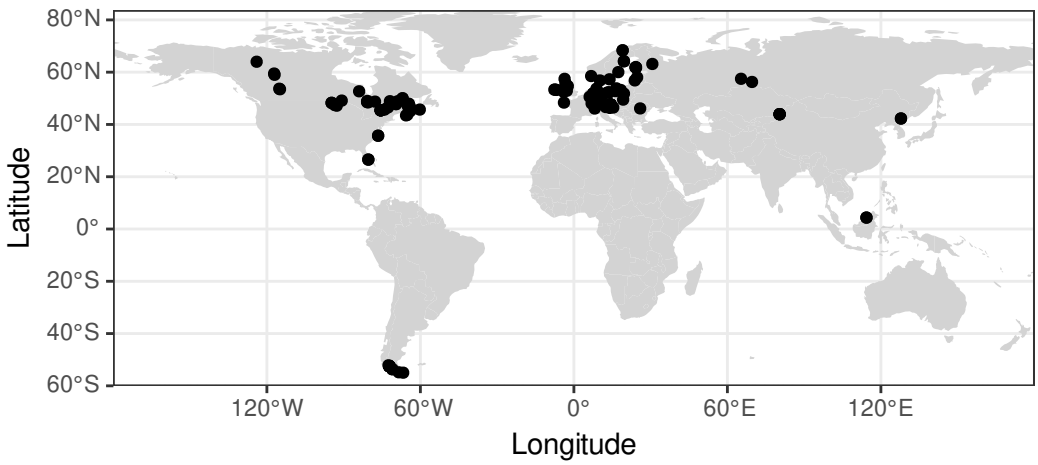

Figure 1: Map of all sampling locations for samples included in the 'pmird' database. Source: https://www.naturalearthdata.com.

Available data formats

For the remaining datasets, data were available as:

1. raw data outputs from measurement devices,

2. processed data outputs from measurement devices (e.g., baseline corrected MIRS, element contents predicted from wavelength-dispersive X-ray fluorescence analysis, etc.),

3. entries in template files specifically developed for the database,

4. custom files, mostly Excel spreadsheets and published manuscripts, created within the respective projects for which the data were originally collected.

Dataset contributions were preferred in the order from 1 to 4. Where possible, raw data were requested directly from data contributors or retrieved from device backups. If only available as PDF, values from data tables were extracted with the 'tabulizer' R package[65]. In a next step, these datasets were reorganized and included in the 'pmird' database.

Database schema

The 'pmird' database was set up as a 'MariaDB' database. The database schema (Fig. 2) was designed to store data and metadata in accordance with classes and elements defined by the Ecological Metadata Language (EML)[66] that were applicable and relevant to the data types and metadata available. General metadata that were considered relevant are geographic, temporal and taxonomic coverage, measurement instruments, and a description of individual methods and method steps[66]. In addition to the EML, discipline- and sample-

or analytic-specific data reporting standards and recommendations were used to decide which data and metadata to include in the 'pmird' database:

1. peat coring and general peat geochemical and physical analysis[67–69]
2. ^{210}Pb, ^{226}Ra, and ^{137}Cs dating[70,71]
3. radiocarbon dating[71]
4. plant macrofossils and testate amoebae[72,73].
5. MIRS: all metadata extractable with the R packages 'hyperSpec'[74] and 'simplerspec'[75] (as implemented in the R packages 'ir'[76] and 'pmird'[77]) were extracted and additional quality variables were defined (see section Technical Validation).

A more detailed description of the database schema is given in section Data Records.

Dataset import and preprocessing

The collected datasets were included into the 'pmird' database using functions from the 'pmird' package[77]. Where MIRS were available as raw data, they were imported including their metadata, using the R packages 'ir'[76], 'hyperSpec'[74], and 'simplerspec'[75]. The metadata collected for MIRS are the metadata extracted with these packages. If metadata were additionally described in articles and reports using the data (for example the number of scans or measurement devices used), these were added. All spectra included in the database were included as received by the data contributors so that no additional preprocessing was applied to the MIRS, but if no raw spectra were available the MIRS may be already preprocessed to some extent.

Other preprocessing steps that were applied are:

1. The recalibration of C and N content data and δ^{13}C and δ^{15}N values using the R package 'elco'[78] — in the case where raw data were available. This calibration does not account for so-called blank effects[79] and therefore the isotope values may be biased (depending on the C or N content and the mass of the sample). Correcting blank effects was not possible because no appropriate correction models could be constructed due to lack of sufficient standard measurements.
2. The recalibration of element contents analyzed by wavelength-dispersive X-ray fluorescence — in case pellet masses used during measurements differed from those used for calibration (also using 'elco'). Measurement errors estimated from these recalibrations are stored alongside the corrected mean values.
3. Unit conversion conducted with the R packages 'units'[80] and 'elco'.

During data import, some samples and data were excluded. These included: (1) samples for which no (approximate) sampling location and (approximate) sampling time were available, (2) corrupted MIRS (broken file format), (3) macrofossil counts where no exact sample volume was available, and (4) data which were not considered as usable in the original projects (e.g., due to measurement errors, device failures, etc.).

An exception was made for data from Liu and Lennartz[26] that report a database of peat

physical and hydraulic properties, albeit without MIRS, sampling locations nor dates. These data were included because they are not published yet, but can be useful to develop prediction models for peat hydraulic properties. None of the data from Liu and Lennartz[26] corresponds to other samples in the database.

In most cases, metadata were available only in the form of published manuscripts, including sampling locations, the description of methods, instruments, settings, and data preprocessing. From these data sources, as much detailed metadata as possible were extracted. In particular, any remarks available on data quality, validation, and processing were included either in the methods description or as comments for individual samples or measurements. In some cases, additional metadata was retrieved from data contributors.

Data Records

The 'pmird' database[25], including the externally stored MIRS data (see below) are made available on Zenodo. In addition, the 'pmird' R package[77], an interface to the 'pmird' database (see section Usage Notes), is also available from Zenodo.

Database schema

The schema of the 'pmird' database is shown in Fig. 2. The database consists of a set of individual tables visualized by boxes which are linked via keys (unique identifiers) listed within the boxes. These links are presented as curves between the tables. A description of the attributes of all tables is presented in Tab. S1.

The top-level table is `datasets`. It stores general information on a dataset, such as the dataset ID, title, year of publication, license, and reference publication. It also includes an identifier that links to the methods used to create the data.

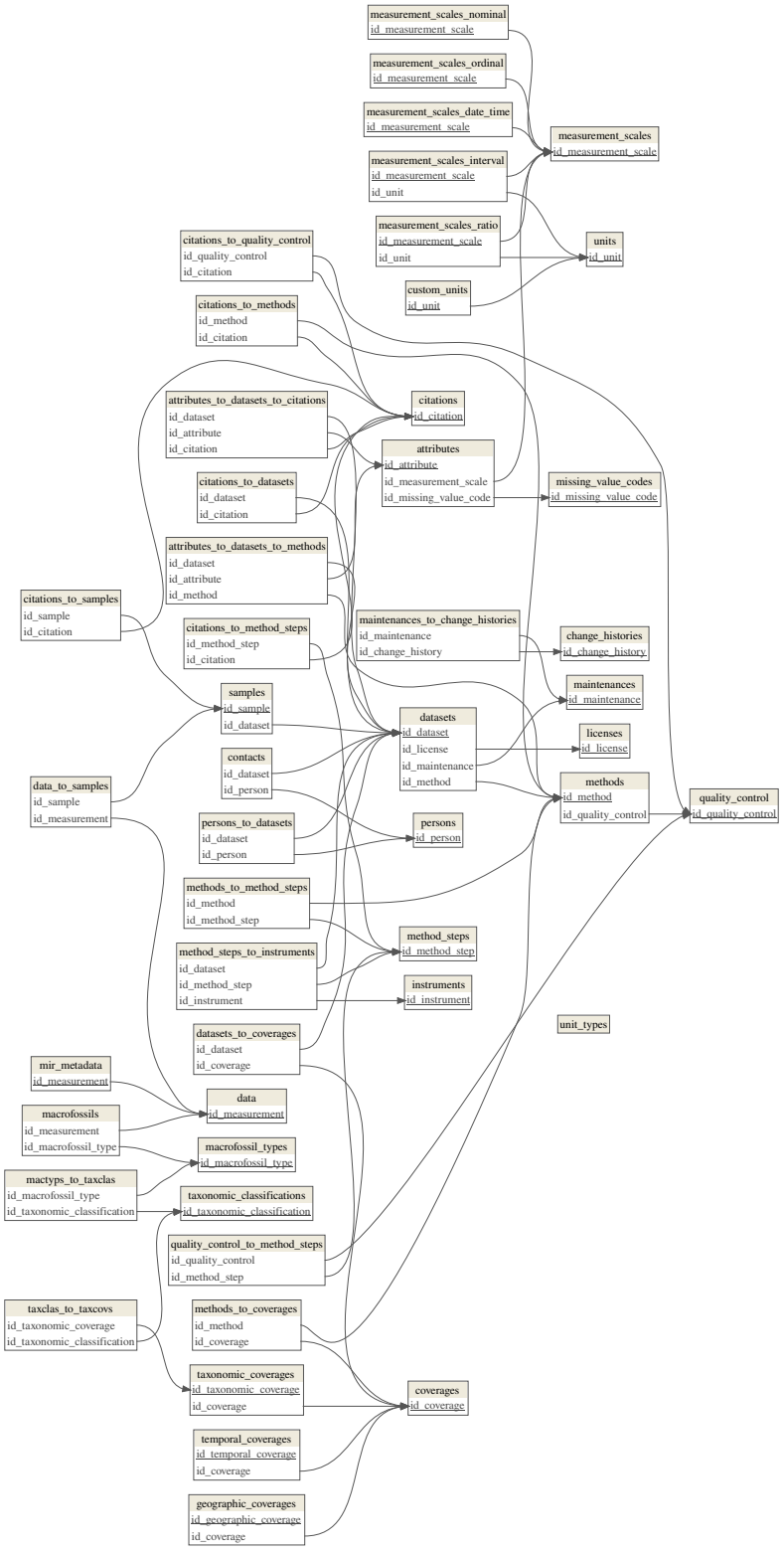

Figure 2: Database schema for 'pmird'. Each table is represented as a box and contain unique identifiers for data entities (e.g. datasets, samples, or measurements) — primary keys (underlined) and foreign keys — which are listed in each box. Keys are used to link data entities between tables. These links are shown as curves pointing to the key in the parent table that is referenced.

Samples

To each dataset, a set of samples in the `samples` table is assigned via the variable `id_dataset`. The table `samples` stores metadata on individual samples collected during a project, such as where and when samples were collected, the sample type (e.g. peat or vegetation), taxonomic information, and the microform (e.g., hummocks, hollows, or lawns) from which the samples were collected. Special metadata or metadata difficult to standardize are stored in the `comments_samples` attribute. The table has a row for each sample indexed by `id_sample`.

Measurements

Attribute values derived from measurements (e.g. element contents, pH, bulk density) are stored in a separate table `data`, where each row represents a measurement and is indexed by `id_measurement`. This format allows storage of replicate measurements on the same sample as are common for some assays or sample collection protocols. The link between measurements and samples is provided via the table `data_to_samples`.

There are three exceptions to this setup: First, MIRS are not stored directly in `data`, but `data` only contains an attribute `mirs_file` that stores the path to the files in the file system where the individual MIRS are stored. Second, MIRS metadata are stored in a separate table `mir_metadata` linked to `data` via `id_measurement`. Third, plant macrofossil and testate amoebae data are stored in a separate table `macrofossils` linked to `data` via `id_measurement` to account for the high diversity in macrofossil attributes (e.g., different taxa, size classes, etc.).

Metadata

Additional metadata on coverage, methods, instruments, and involved persons are stored in separate tables. Each dataset has coverage information, including geographic coverage (a bounding box for the sampling locations and a description of the sampling locations; table `geographic_coverages`), temporal coverage (time point or range of the data collection; table `temporal_coverages`), and taxonomic coverage (taxa included in the dataset; table `taxonomic_coverages`). In cases where only the sampling year was known, the month and day were set to January 1 of that year. Such cases have a corresponding note in column `comments_samples`.

Each dataset has a detailed method description in several rows in the table `methods`. For each dataset, the first row contains a description of the sample collection and — if applicable, sampling design or experimental design. This row is linked to the table `method_steps` (via table `methods_to_method_steps`) where individual steps for all applied methods (if applicable) are described (e.g., drying, milling, MIRS measurements, measurements of elemental contents, plant macrofossil analysis, dating, etc.). An example of such a description is shown in Tab. S2.

In addition, table `attributes_to_datasets_to_methods` links individual methods for each dataset to the specific attributes they refer to (e.g., C content) to avoid ambiguity over which methods were used to measure a specific attribute.

Instruments used for data collection are listed in table `instruments` and linked to indi-

vidual method steps in table `method_steps` via table `method_steps_to_instruments`. Finally, information on units for all attributes are stored in various tables linked by table `measurement_scales`.

Technical Validation

All datasets were validated on two levels: a validation within the projects in which the data were originally created, and a validation prior inclusion in the database. Available information on the technical validation for each dataset is given within the `methods` and `method_steps` tables (Fig. 2).

Validation within individual projects

The 'pmird' database combines heterogeneous datasets collected within different individual projects. For different attributes, the extent to which community standards for validation procedures exist is highly variable. For instance, peat dating typically has highly standardized validation procedures because measurements are performed by highly specialized laboratories with standardized protocols, whereas no single, widely adopted standard exists for example for bulk density measurements or for the measurement of MIRS. For these reasons, validation procedures, the extent to which these are reported, and data quality vary between datasets.

Validation of datasets during import

As described in the section Collection of suitable datasets, a minimal quality check was whether sufficient metadata were available to provide basic information on the methods used (including instruments used, sample processing, sampling location and date). Due to the legacy nature of many datasets, an independent, full technical validation could not be performed, because in many cases raw data or information on data processing were not available.

Raw data (including standard measurements) were available for only a few datasets, and only for C and N contents and stable isotope signatures. In these cases, the calibration was checked and updated where necessary and possible and the corresponding estimated measurement errors were included in the database.

Validation of mid-infrared spectra

We computed several quality indicators to check the quality of the MIRS: it was checked whether the imported spectra were baseline corrected and we estimated the relative contribution of water vapor or CO_2 artifacts, and signal noise. These quality indicators can be used to filter MIRS in the 'pmird' database.

Below, we describe how the quality indicators were computed. All MIRS validation procedures make use of the following variables:

1. $X_{\mathbf{1}}$: The set of all MIRS interpolated with `ir::ir_interpolate()` with parameter `dw` set to 1.

2. A(X_1): A vector that stores the sum of the intensity values of each spectrum in $X_{\mathbf{1}}$ after (1) clipping $X_{\mathbf{1}}$ to the range [699, 3999] cm^{-1}, (2) linearly interpolating the region of the CO_2 peaks ([2250, 2450] cm^{-1}) to avoid corrupted baselines due to negative CO_2 peaks, (3) baseline correction using `ir::ir_bc_rubberband()`.

Definition of reference spectra

We quantified water vapor and CO_2 artifacts using reference spectra of pure water vapor and CO_2 (Fig. 3). The general procedure is to scale these reference spectra to a selected portion of the spectra which contains only water vapor or CO_2 peaks (Fig. 4). The so computed scale factor is an estimate for the relative contribution of water vapor and CO_2, respectively. Ideally, the spectra of pure water vapor and CO_2 gas would be measured on each used device on which the (peat) sample MIRS were measured[81]. However, no such data were available. When background scans were present, we derived equivalent data for CO_2 from raw MIRS according to the following procedure:

1. Selection: Select two background spectra recorded on the same device and preferentially on the same day (with intensities recorded as transmission) which were recorded under different CO_2 concentrations, but similar water vapor concentrations. The differences can be inferred from the relative magnitude of peaks which are known to be caused by water vapor and CO_2, respectively[82,83]. Since we are only interested in an approximate estimation of the relative contribution of CO_2, remaining small differences in water vapor concentrations were negligible (Fig. 3).

2. Calculation: Compute the spectrum for pure CO_2 by dividing the intensity values of both spectra. This spectrum is converted to absorbance values.

3. Preprocessing: Perform additional preprocessing steps to make the spectra usable for the estimation and potential correction tasks: (1) interpolate the spectrum to integer wavenumber values increasing by 1 cm^{-1}, (2) replace the regions 728 to 2230 cm^{-1} and > 3800 cm^{-1} with straight lines (this was done to remove remaining noise and water vapor artifacts from regions known not to contain peaks caused by CO_2, only in case such artifacts were visible in the resulting spectra[82,83]), and (3) baseline correct the spectra.

For water vapor, the procedure to obtain an approximately pure water vapor spectrum is the same as for CO_2, with the following differences: In step 3 above, no regions of the water vapor spectrum are replaced by straight lines. Moreover, the following additional steps were performed (after step 3 above):

4. Atmospheric correction: Use the respective pure CO_2 spectrum to perform an atmospheric correction as elsewhere suggested[84]. This was done because CO_2 concentrations differed to some extent between the available background spectra. This correction was only partly successful, but sufficient to obtain an approximately pure water vapor spectrum for our purposes.

Table 2: Overview on the devices with which data to compute the reference spectra were measured ("Source device") and for data from which devices these reference spectra are used to estimate the relative contribution of water vapor and CO_2 artifacts ("Target device").

Source device	Target device
Bruker Vector 22 FTIR spectrometer (Bruker Optik, Ettlingen, Germany)	Bruker Vector 22 FTIR spectrometer (Bruker Optik, Ettlingen, Germany) Shimadzu IRTracer-100 spectrophotometer, equipped with a DLaTGS (deuterated L-alaninedoped triglycine sulfate) detector PerkinElmer Spectrum 100 FTIR spectrometer
Cary 670 FTIR spectrometer (Agilent, Santa Clara, CA, USA)	Cary 660 FTIR spectrometer (Agilent, Santa Clara, CA, USA) Varian 670 FTIR spectrometer (Agilent, Palo Alto, USA) Cary 670 FTIR spectrometer (Agilent, Santa Clara, CA, USA) Cary 600 FTIR spectrometer (Agilent, Santa Clara, CA, USA) Varian 660 FTIR spectrometer (Agilent, Palo Alto, USA)

5. Remaining negative intensity values were removed by dividing the intensity values such that the background at 2000 cm^{-1} had an intensity of 1, then subtracting 1 from the intensity values, and finally setting all values < 0 to 0. Remaining CO_2 artifacts and noise were removed by replacing the regions 600 to 1200 cm^{-1} and 2200 to 3300 cm^{-1} with straight lines.

The resulting spectra (Fig. 3) have key characteristics of pure water vapor (https://webbook.nist.gov/cgi/inchi?ID=C7732185&Type=IR-SPEC&Index=0) and CO_2 spectra (https://webbook.nist.gov/cgi/cbook.cgi?ID=C124389&Type=IR-SPEC&Index=1) as contained in the NIST/EPA Gas-Phase Infrared Database[82,83].

Such reference spectra could not be computed for every device used to measure MIRS in the 'pmird' database due to missing raw data. For this reason, we used reference spectra computed from data from different devices as reference spectra for other devices. Reference spectra could only be computed for absorbance spectra, but not ATR spectra. As a consequence, water vapor and CO_2 MIRS artifacts in ATR spectra are estimated using reference spectra measured in absorbance mode which introduces larger errors to our estimates in these cases. An overview of the assignment of reference spectra to devices is given in Tab. 2.

Identification of baseline corrected spectra

Different device settings, sample amounts, and internal scattering result in different baseline absorbances recorded during MIRS measurements[81]. Baseline correction is a heuristic procedure to subtract such differences in the baseline absorbance and thus is typically required to compare spectra of different samples[81].

However, since baseline correction strongly depends on the specific spectra (e.g., the spectral range) and the occurrence of water and CO_2 artifacts, and since different baseline procedures exist and more suitable algorithms may be developed in the future, it is preferable to publish unprocessed spectra.

Raw spectra were not available for all datasets in the 'pmird' database, as often only already baseline corrected data were available. Since these spectra can nevertheless be useful, they were not excluded. A further problem is that information on whether a spectrum had been already baseline corrected was unavailable, except when stated in published articles.

To identify spectra that were already baseline corrected, we used the fact that MIRS of organic matter typically have a baseline that decreases from the smallest MIR wavenumber ranges (~ 400 cm^{-1}) to ~2300 cm^{-1}. Thus, non-baseline corrected spectra have large baseline absorbances at lower wavenumber values, whereas already baseline corrected spectra have small baseline absorbances in this region.

We used the following procedure to detect spectra that were already baseline corrected:

1. Compute $\mathbf{X_2}$: Take $\mathbf{X_1}$, (1) interpolate linearly the region of the CO_2 peaks (as described above), (2) perform the rubberband baseline correction as described above, but return the baseline instead of the baseline corrected spectra, (3) clip the baselines to the region [1400, 3400] cm^{-1} to get a uniform reference range (this is important to get homogeneous results after normalization in the following step, Fig. 4), and (4) divide the resulting baseline absorbances by $A(X_1)$.

2. Compute $I_{1400}(\mathbf{X_2})$: Extract from $\mathbf{X_2}$ the normalized intensity at 1400 cm^{-1}.

3. Define the logical vector `is_baseline_corrected` which is `TRUE` whenever $I_{1400}(\mathbf{X_2}) > t_{bc}$ and otherwise `FALSE`, where t_{bc} is set to 9×10^{-5}. `is_baseline_corrected` is stored in the table `mir_metadata` in the database.

The value of t_{bc} was defined based on visual inspection of Fig. 5 (a) which shows $I_{1400}(\mathbf{X_2})$ versus the MIRS measurement number in the 'pmird' database. Differences between datasets are clearly visible, as well as between baseline corrected spectra which have values near zero and non-baseline corrected spectra which have larger values than t_{bc}. t_{bc} was not set to a smaller value because dataset 1 (containing ATR-FTIR spectra) contains baseline corrected spectra[27], but has higher values for $I_{1400}(\mathbf{X_2})$ due to noise.

Water vapor artifacts

Water vapor causes a range of artifact peaks in MIRS due to differences in the atmospheric water content during sample measurements in comparison to background measurements[81]. Water vapor artifacts can distort peaks from organic matter across broad regions of the MIRS[81]. High quality spectra have small water vapor peaks. To detect water vapor peaks,

we focused on the range [3780, 3920] cm^{-1}, where a series of water vapor peaks can be observed[81,82], whilst organic matter typically causes no peaks in this range[85,86] (Fig. 4). We used the following procedure to estimate the relative contribution of water vapor to the MIRS:

1. Compute $X_{\mathbf{3}}$: Process $X_{\mathbf{1}}$ with `pmird::pm_ir_extract_peak()` with `range` set to [3780, 3920] cm^{-1}, and `peak_max` to 3853 cm^{-1}. This clips $X_{\mathbf{1}}$ to the defined water vapor region and baseline corrects the region conditional on whether water vapor artifacts are negative (less water vapor contribution in the sample spectrum in comparison to the background spectrum) or positive (more water vapor contribution in the sample spectrum in comparison to the background spectrum). Finally, normalize the intensities by division by $A(X_1)$.

2. Define x_{wv}: A reference spectrum from $X_{\mathbf{3}}$ as described above in section Definition of reference spectra.

3. Define c_{wv}: For each spectrum in $X_{\mathbf{3}}$, model the intensities with the intensities in x_{wv} using ordinary least squares regression, and extract the slope of the regression line (average and standard error).

c_{wv} is the relative contribution of water vapor to each spectrum in the database and $SE(c_{wv})$ the standard error. For x_{wv}, $c_{wv} = 1$. For a spectrum with no water vapor artifacts, $c_{wv} \approx 0$. For spectra with negative water vapor artifacts, $c_{wv} < 0$, and for spectra with positive water vapor artifacts, $c_{wv} > 0$. An overview on the values of c_{wv} for all spectra is given in Fig. 5 (b). c_{wv} is stored as `mir_water_vapor_contribution_relative` in the table `mir_metadata` in the database, and $SE(c_{wv})$ as `mir_water_vapor_contribution_relative_sd`.

CO_2 artifacts

CO_2 causes a range of artifact peaks in MIRS due to differences in the atmospheric CO_2 concentration during sample measurements in comparison to background measurements[82,84]. CO_2 artifacts can distort peaks from organic matter particularly around ca. 600 to 750, 2250 to 2400, and 3500 to 3700 cm^{-1}[82,83]. High quality spectra have small CO_2 peaks. To detect CO_2 peaks, we focused on the range [2250, 2450] cm^{-1}, where a series of CO_2 peaks can be observed[82,83], whilst organic matter typically causes no peaks in this range[85,86] (Fig. 4). We used the following procedure to estimate the relative contribution of CO_2 to the MIRS:

1. Compute $X_{\mathbf{4}}$: Process $X_{\mathbf{1}}$ with `pmird::pm_ir_extract_peak()` with `range` set to [2250, 2450] cm^{-1}, and `peak_max` to 2362 cm^{-1}. This clips $X_{\mathbf{1}}$ to the defined CO_2 region and baseline corrects the region conditional on whether CO_2 artifacts are negative (less CO_2 contribution in the sample spectrum in comparison to the background spectrum) or positive (more CO_2 contribution in the sample spectrum in comparison to the background spectrum). Finally, normalize the intensities by division by $A(X_1)$.

2. Define x_{CO_2}: A reference spectrum from $X_{\mathbf{4}}$ as described above in section Definition of reference spectra.

3. Define c_{CO_2}: For each spectrum in $X_{\mathbf{4}}$, model the intensities with the intensities in

x_{CO_2} using ordinary least squares regression, and extract the slope of the regression line (average and standard error).

c_{CO_2} is the relative contribution of CO_2 to each spectrum in the database and SE(c_{CO_2}) the standard error. For x_{CO_2}, $c_{CO_2} = 1$. For a spectrum with no CO_2 artifacts, $c_{CO_2} \approx 0$. For spectra with negative CO_2 artifacts, $c_{CO_2} < 0$, and for spectra with positive CO_2 artifacts, $c_{CO_2} > 0$. An overview on the values of c_{CO_2} for all spectra in the database is given in Fig. 5 (c). c_{CO_2} is stored as `mir_co2_contribution_relative` in the table `mir_metadata` in the database, and SE(c_{CO_2}) as `mir_co2_contribution_relative_sd`.

Noise

MIRS intensities can have contributions from signal noise e.g. in dependency of the number of scans averaged per spectrum, the sensor, and the MIR radiation source[81]. Noise can distort peaks and can cause differences in baseline correction, as well as the identification of water vapor and CO_2 artifacts. We estimated the relative noise contribution as the variance of intensity values around the average intensity in a spectrum in a region without sharp peaks. For this, we focused on the range [2700, 2750] cm^{-1} (Fig. 4), which has no sharp peaks caused by organic matter and is less impacted by water vapor than other regions without sharp peaks in organic matter MIRS.
We used the following procedure to estimate the relative contribution of noise to the MIRS:

1. Define c_{noise}: The variance of intensity values in $X_{\mathbf{1}}$ after (1) clipping $X_{\mathbf{1}}$ to the range [699, 3999] cm^{-1}, (2) interpolating linearly the region of the CO_2 peaks ([2250, 2450] cm^{-1}) — to avoid corrupted baselines due to negative CO_2 peaks —, (3) baseline correction using `ir::ir_bc_rubberband()`, (4) Savitzky-Golay baseline correction to estimate the average intensity of a spectrum, (5) Normalization of intensity values by dividing them by their sum, (6) clipping to the noise range ([2700, 2750] cm^{-1}), and (7) computation of the variance of the intensity values.

If $c_{noise} \approx 0$, no noise is detected in the spectrum and the larger c_{noise} is, the larger is the relative contribution of noise. An overview on the values of c_{noise} for all spectra is given in Fig. 5 (d). c_{noise} is stored as `noise_level_relative` in the table `mir_metadata` in the database.

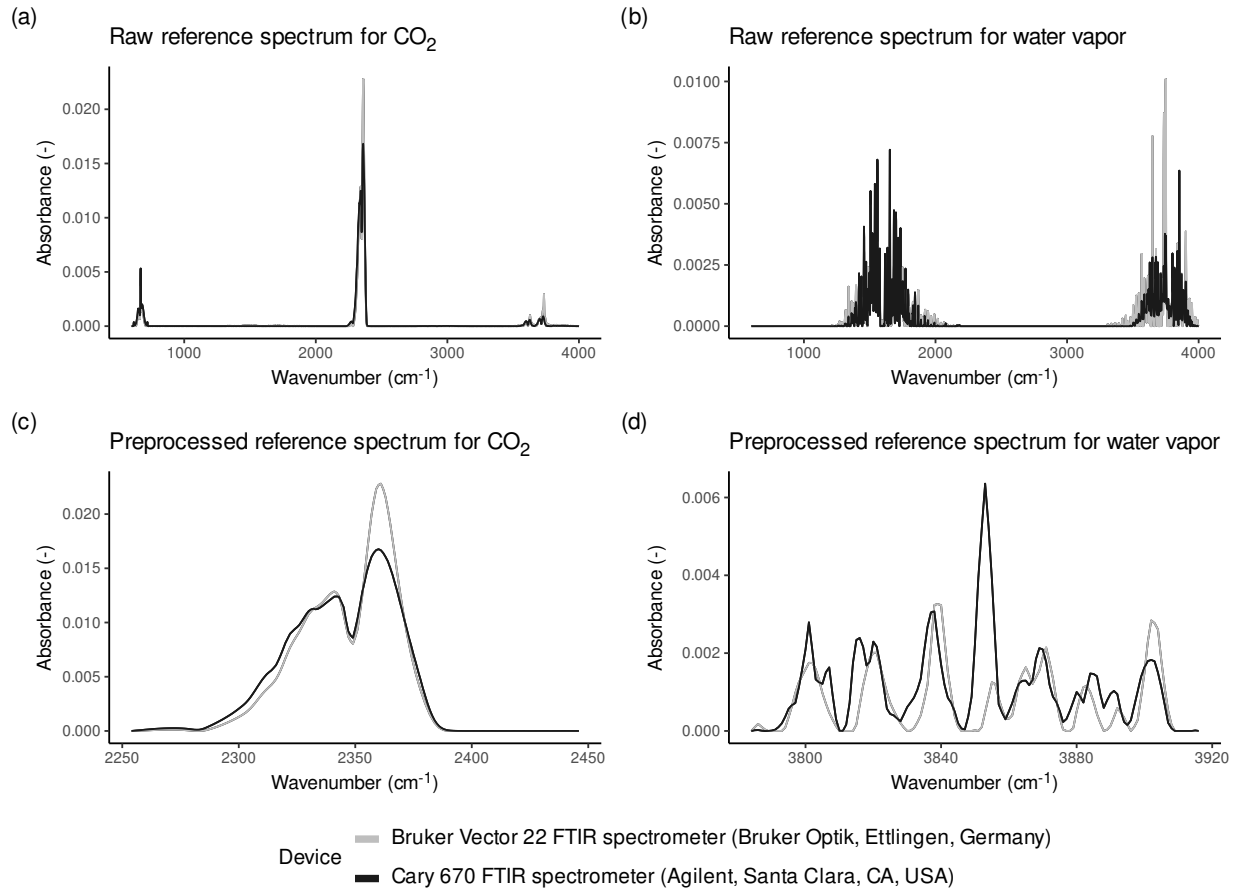

Figure 3: The raw and preprocessed reference spectra used to estimate the relative contribution of CO_2 and water vapor to the spectra in the 'pmird' database. The preprocessed spectra (bottom row) correspond to x_{CO_2} and x_{wv}, respectively. The top row shows the same spectra before preprocessing. Colors indicate the measurement devices on which the spectra were recorded.

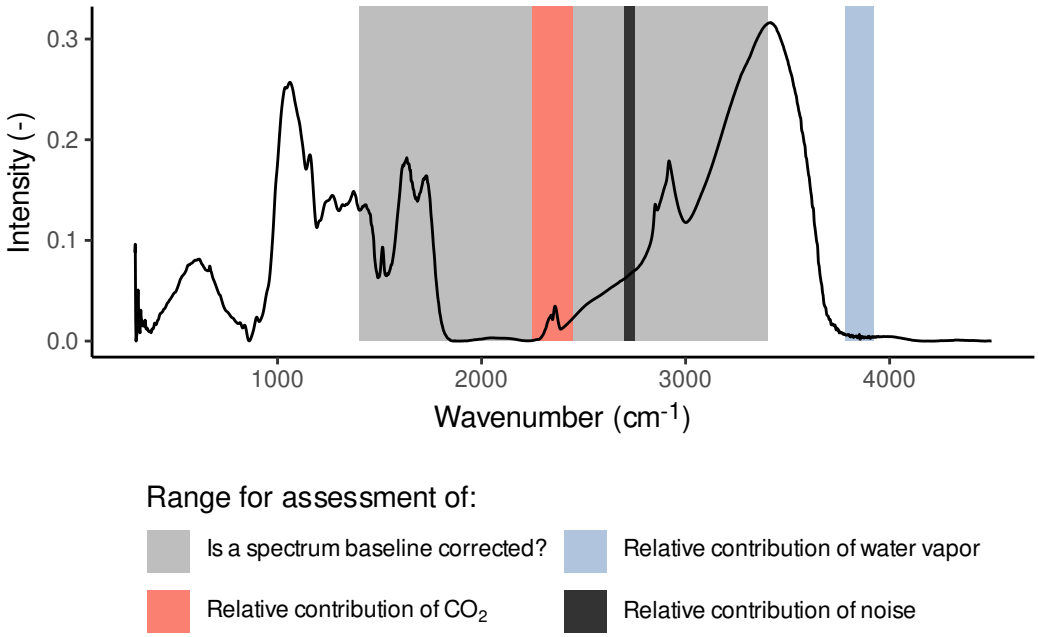

Figure 4: A sample spectrum from the 'pmird' database with the spectral ranges used during assessment of the quality attributes highlighted. For "Is a spectrum baseline corrected?", the region of the spectra is clipped to [1400, 3400] cm^{-1}. To assess the relative contribution of water vapor, the range [3780, 3920] cm^{-1} is considered. To assess the relative contribution of CO_2, CO_2 peaks in the range [2250, 2450] cm^{-1} are considered. To assess the relative contribution of noise, the range [2700, 2750] cm^{-1} is considered.

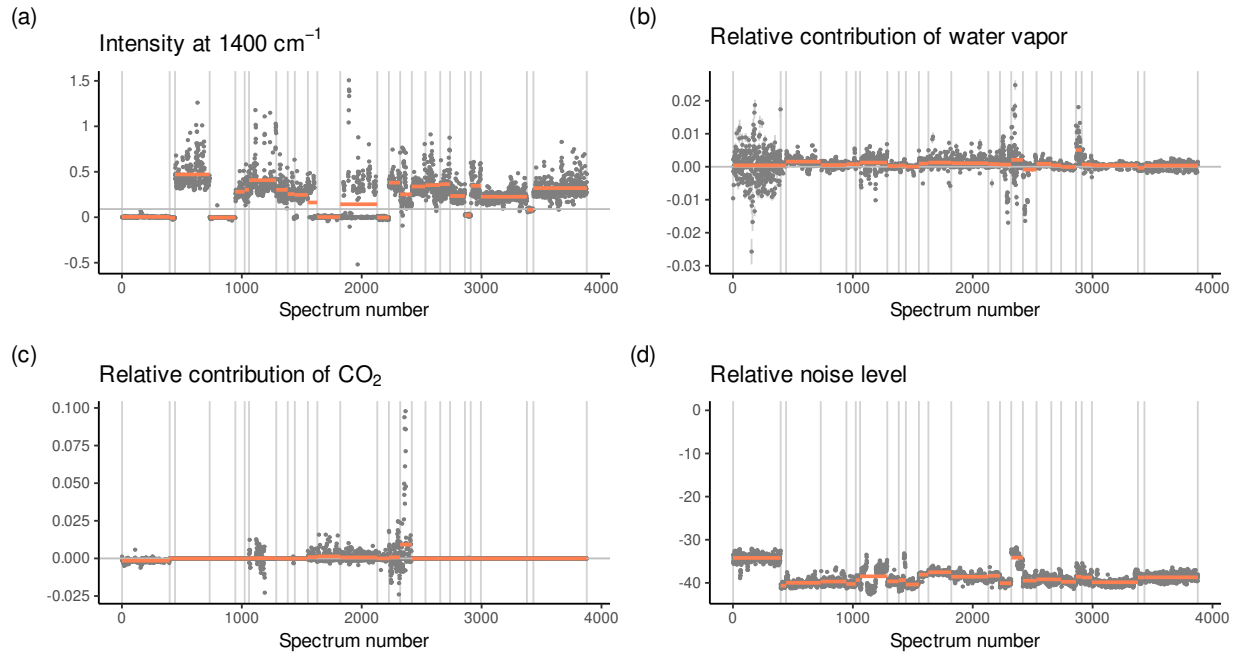

Figure 5: Data quality assessment for the spectra in the 'pmird' database. For each validation step described in section Validation of mid-infrared spectra, the values of the defined variable to assess the quality of the spectra are shown for each spectrum. Spectra are listed in the order of their appearance in the 'pmird' database along the horizontal axis. Vertical lines represent the first and last spectrum in a dataset. Red horizontal lines are the dataset averages. Error bars represent standard errors for estimated contributions of water vapor and CO_2. (a) Intensity of the baseline of the spectra at 1400 cm^{-1} ($I_{1400}(X_{\mathbf{2}})$). This variable is used to identify baseline corrected spectra. The horizontal grey line denotes the threshold value (t_{bc} =9×10^{-5}) used to differentiate baseline corrected spectra (below the line) from non-baseline corrected spectra (above the line). For illustrative purposes, all values along the vertical axis are multiplied by 1000. (b) Relative contribution of water vapor to the spectra (c_{wv}, `mir_water_vapor_contribution_relative` in table `mir_metadata`). (c) Relative contribution of CO_2 to the spectra (c_{CO_2}, `mir_co2_contribution_relative` in table `mir_metadata`). (d) Relative contribution of noise to the spectra (c_{noise}, `noise_level_relative` in table `mir_metadata`). For illustrative purposes, all values along the vertical axis are log transformed.

Usage Notes

The 'pmird' database can be downloaded from Zenodo[25]. The downloaded data contain a database backup (pmird-backup-2025-09-10.sql) and raw MIRS data files in the folder `pmird_prepared_data`. The database backup needs to be imported to a 'MariaDB' server, the folder `pmird_prepared_data` can be stored at any location. In a linux terminal, the downloaded database backup can be imported like so:

```
mysql -u<user> -p pmird < pmird-backup-2025-09-10.sql
```

Here, `<user>` is the user for the 'MariaDB' server. More information on 'MariaDB' can be found here: https://mariadb.com/.
Data can be accessed for example via 'MariaDB', or via R[87] with the 'RMariaDB' package[88].
An R package that provides functions to access and manipulate the database, 'pmird'[77], has also been developed. The following use cases illustrate how to access the database with the 'pmird' package and what additional packages may be useful to analyze data exported from the database, in particular the spectra.

Database access via the 'pmird' R package

The 'pmird' R package can be downloaded and installed from GitHub using the remotes package[89]. Other packages needed for this tutorial are also installed:

```r
# installation
remotes::install_github("henningte/pmird")

# installation of other packages
install.packages("magrittr")
install.packages("RMariaDB")
remotes::install_github("henningte/ir")
remotes::install_github("henningte/irpeat")

# load needed packages for this tutorial
library(pmird)
library(ir)
library(irpeat)
```

Once the database is set up and runs in a 'MariaDB' instance (see previous subsection), it can be accessed from within R, using the 'RMariaDB' package[88]:

```r
# connect to database
con <-
  RMariaDB::dbConnect(
    drv = RMariaDB::MariaDB(),
    dbname = "pmird",
    default.file = "~/my.cnf",
    groups = "rs-dbi"
  )
```

Here, `my.cnf` is a text file that stores user and password information for the database server. From here on, the 'pmird' R package can be used to access the database. The 'pmird' R package makes use of the R package 'dm'[90] to access and manipulate the database contents. `pmird::pm_get_dm()` creates a `dm` object which stores the database structure.

```r
# create the dm object
dm_pmird <- pmird::pm_get_dm(con, learn_keys = TRUE)
```

The option `learn_keys = TRUE` means that information on the primary and foreign key is added to the dm object. A `dm` object is a representation of the entire database and allows comfortable manipulation of the database from within R (e.g. addition of new rows to tables, addition of new tables, data queries)[90].

Use case: obtaining general information on the datasets contained in the 'pmird' database

General information on the datasets contained in the 'pmird' database is stored in table `datasets`. The 'pmird' R package provides a function to obtain this table from the `dm` object (`pmird::pm_get_table(.table_name = "datasets")`).

```r
# extract the datasets table
pmird_datasets <-
  dm_pmird |>
  pmird::pm_get_table(.table_name = "datasets")
```

This table can, for example, be used to select studies to extract data from the 'pmird' database.

Use case: extracting data for a specific dataset from the 'pmird' database

Assume you are interested in viewing all measured data for one specific dataset, e.g. the dataset with `id_dataset == 8` in `pmird_datasets`. Using the 'dm' package and the `dm` object representing the 'pmird' database (`dm_pmird`), these data can be obtained as follows:

```r
# get data for the dataset with ID 8
d8 <-
  dm_pmird |>
  dm::dm_zoom_to(datasets) |>
  dm::filter(id_dataset == 8) |>
  dm::left_join(samples, by = "id_dataset") |>
  dm::left_join(data_to_samples, by = "id_sample") |>
  dm::left_join(data, by = "id_measurement") |>
  dm::left_join(mir_metadata, by = "id_measurement") |>
  dm::left_join(macrofossils, by = "id_measurement") |>
  dm::pull_tbl() |>
  tibble::as_tibble()
```

The resulting data frame (`d8`) contains information on all samples and measurements for the dataset with `id_dataset == 8`. `d8` does not yet contain any spectra, but stores only information on the respective file paths to the downloaded spectra files within the downloaded

folder `pmird_prepared_data`.
To load the spectra, you can use the function `pmird::pmird_load_spectra()`. In addition, you have to specify via argument `directory` in which folder `pmird_prepared_data` is stored (on the computer used for this tutorial, this was `"data/derived_data/"`):

```
# load the spectra
d8 <- pmird::pm_load_spectra(d8, directory = "data/derived_data/")
```

`pm_load_spectra()` is a wrapper function around functions from the package 'ir'[76] which in turn are wrappers around `read.spc()`[74] and `read.csv()`. `pm_load_spectra()` therefore can load spectra both saved as spc and csv files. `pm_load_spectra()` also converts `d8` into an object of class `ir` from the 'ir' package. 'ir' provides functions for spectral preprocessing and manipulation[76] and is compatible with the 'irpeat' package which provides functions to analyze peat MIRS and spectral prediction models to predict peat properties from MIRS[91].

Use case: spectral preprocessing workflow

Here, an example workflow to preprocess the spectra in `d8` with the R package 'ir' is shown. The workflow assumes high quality MIRS and therefore does not correct noise, water vapor or CO_2 artifacts. The workflow has the following steps:

1. Linear interpolation (When specifying wavenumbers, for example during clipping, 'ir' warns about any numeric deviations. Linear interpolation avoids these warnings).
2. Clipping to the wavenumber range of interest.
3. Baseline correction using a convex hull[74].
4. Normalization by dividing all intensity values by the sum of all intensity values.

Which map to the following code:

```
# define the clipping range
clip_range <-
  data.frame(
    start = 650,
    end = 3990,
    stringsAsFactors = FALSE
  )

# typical preprocessing workflow
d8_preprocessed <-
  d8 |>
  ir::ir_interpolate(start = NULL, dw = 1) |>  # linear interpolation
  ir::ir_clip(range = clip_range) |>           # clipping
  ir::ir_bc(                                   # baseline correction
    method = "rubberband",
    do_impute = TRUE
  ) |>
  ir::ir_normalize(method = "area")            # normalization
```

A comparison of the loaded spectra before and after preprocessing is shown in Fig. 6.

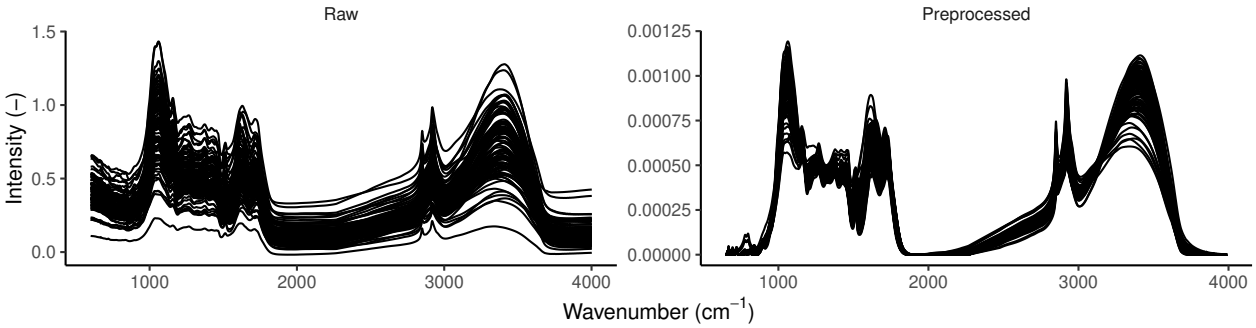

Figure 6: Comparison of the spectra for the dataset `d8` extracted from the 'pmird' database before and after applying the preprocessing workflow described in section Use case: spectral preprocessing workflow.

Use case: computation of humification indices and spectral prediction models

Here, computation of humification indices[11,12,45] with the 'irpeat' package is shown:

```
# compute a humification index
d8_preprocessed <-
  d8_preprocessed |>
  irpeat::irp_hi(x1 = 1630, x2 = 1090)

# show some values
head(d8_preprocessed$hi_1630_1090, 3)
```

```
## [1] 0.4653120 0.4507052 0.8271826
```

The 'irpeat' package contains, for example, a prediction model for the electron accepting capacity[42] that can be applied to raw MIRS (for further details, please see the documentation of the 'irpeat' package):

```
d8_eac <-
  d8 |>
  dplyr::filter(! ir::ir_identify_empty_spectra(d8)) |>
  irpeat::irp_eac_1(do_summary = TRUE)

# show some values
head(d8_eac$eac, 3)
```

```
## Units: [umol/g]
## Errors: 172.0593 168.4222 191.2435
##        1        2        3
## 611.5772 536.4737 805.5097
```

Use case: Handling units and measurement errors

The R package 'quantities'[80,92] can be used to add units and measurement errors to measured variables from the 'pmird' database. The 'pmird' R package allows batch unit and measurement error assignment:

```
# add information on units and errors with the 'quantities' package
d8 <-
  d8 |>
  pmird::pm_add_quantities()

# show some values
head(d8$N, 3)
```

```
## Units: [g/g]
## Errors: 0.0000996441 0.0001036096 0.0001168346
## [1] 0.014054321 0.007934011 0.021408554
```

Use case: Generating data citations

Whoever uses data from the 'pmird' database should cite, in addition to the database, the original data sources for the used datasets. To make this straightforward, the 'pmird' R package contains the function `pm_get_citations()` to generate such a citation list for any extracted data subset:

```
# collect all citations for `d8`:
d8_citations <-
  pm_get_citations(
    con = con,
    x = d8$id_measurement,
    file = "d8_citations.bib"
  )
```

```
## Loading required namespace: bib2df
```

```
# close connection to database
RMariaDB::dbDisconnect(con)
```

The function takes column `id_measurement` of the extracted data and collects citations for all relevant data sources from the database. The results are exported to a bibtex file which is defined via argument `file`. This file can be imported to literature reference software. In this case, since the data have not been previously published, the created bibtex file is empty. `RMariaDB::dbDisconnect(con)` closes the connection to the database, as this is the final use case presented here.

Data availability

The Peatland Mid-Infrared Database is available from Zenodo (https://doi.org/10.5281/zenodo.17092587)[25].

Code availability

All code used to create the 'pmird' database is available within the repository of the 'pmird' database[25]. Detailed information about how these scripts work together can be found in the README file in the repository. The underlying data cannot be made available because some of them contain personal data. Therefore, the database cannot be reproduced from scratch. The 'pmird' R package is available from Zenodo[77]. Code to reproduce this manuscript is available from GitHub[93].

Acknowledgements

This study was funded by the Deutsche Forschungsgemeinschaft (DFG, German Research Foundation) grant no. KN 929/23-1 to Klaus-Holger Knorr and grant no. PE 1632/18-1 to Edzer Pebesma. We thank Chuanyu Gao for measuring electron accepting and donating capacities that were obtained from[42]. For dataset-specific acknowledgements, please refer to the information on acknowledgements stored in the 'pmird' database.

Author contributions statement

HT: Conceptualization, methodology, software, validation, formal analysis, investigation, visualization, writing - original draft. KHK: supervision, funding acquisition. All authors: data curation, writing - review & editing

Competing interests

The authors declare no competing interests.

References

1. Loisel, J. *et al.* A database and synthesis of northern peatland soil properties and Holocene carbon and nitrogen accumulation. *The Holocene* **24**, 1028–1042 (2014).

2. Yu, Z., Loisel, J., Brosseau, D. P., Beilman, D. W. & Hunt, S. J. Global peatland dynamics since the Last Glacial Maximum. *Geophysical Research Letters* **37**, 2010GL043584 (2010).

3. Nichols, J. E. & Peteet, D. M. Rapid expansion of northern peatlands and doubled estimate of carbon storage. *Nature Geoscience* **12**, 917–921 (2019).

4. Xu, J., Morris, P. J., Liu, J. & Holden, J. PEATMAP: Refining estimates of global peatland distribution based on a meta-analysis. *CATENA* **160**, 134–140 (2018).

5. Blodau, C. Carbon cycling in peatlands A review of processes and controls. *Environmental Reviews* **10**, 111–134 (2002).

6. Frolking, S. *et al.* Peatlands in the Earth's 21st century climate system. *Environmental Reviews* **19**, 371–396 (2011).

7. Serk, H. *et al.* Organochemical characterization of peat reveals decomposition of specific hemicellulose structures as the main cause of organic matter loss in the acrotelm. *Environmental Science & Technology* **0**, null (2022).

8. Heitmann, T. & Blodau, C. Oxidation and incorporation of hydrogen sulfide by dissolved organic matter. *Chemical Geology* **235**, 12–20 (2006).

9. Gao, C., Sander, M., Agethen, S. & Knorr, K.-H. Electron accepting capacity of dissolved and particulate organic matter control CO_2 and CH_4 formation in peat soils. *Geochimica et Cosmochimica Acta* **245**, 266–277 (2019).

10. Pierce, C. E. *et al.* Role of ester sulfate and organic disulfide in mercury methylation in peatland soils. *Environmental Science & Technology* **56**, 1433–1444 (2022).

11. Niemeyer, J., Chen, Y. & Bollag, J.-M. Characterization of humic acids, composts, and peat by diffuse reflectance Fourier-transform infrared spectroscopy. *Soil Science Society of America Journal* **56**, 135–140 (1992).

12. Beer, J., Lee, K., Whiticar, M. & Blodau, C. Geochemical controls on anaerobic organic matter decomposition in a northern peatland. *Limnology and Oceanography* **53**, 1393–1407 (2008).

13. Biester, H., Knorr, K.-H., Schellekens, J., Basler, A. & Hermanns, Y.-M. Comparison of different methods to determine the degree of peat decomposition in peat bogs. *Biogeosciences* **11**, 2691–2707 (2014).

14. Artz, R. R. E. *et al.* FTIR spectroscopy can be used as a screening tool for organic matter quality in regenerating cutover peatlands. *Soil Biology and Biochemistry* **40**, 515–527 (2008).

15. Chapman, S. J., Campbell, C. D., Fraser, A. R. & Puri, G. FTIR spectroscopy of peat in and bordering Scots pine woodland: Relationship with chemical and biological properties. *Soil Biology and Biochemistry* **33**, 1193–1200 (2001).

16. Helfenstein, A. *et al.* Quantifying soil carbon in temperate peatlands using a mid-IR soil spectral library. *SOIL* **7**, 193–215 (2021).

17. Nocita, M. *et al.* Prediction of soil organic carbon content by diffuse reflectance spectroscopy using a local partial least square regression approach. *Soil Biology and Biochemistry* **68**, 337–347 (2014).

18. Viscarra Rossel, R. A. *et al.* A global spectral library to characterize the world's soil. *Earth-Science Reviews* **155**, 198–230 (2016).

19. Cardelli, V. *et al.* Non-saturated soil organic horizon characterization via advanced proximal sensors. *Geoderma* **288**, 130–142 (2017).

20. Orgiazzi, A., Ballabio, C., Panagos, P., Jones, A. & Fernández-Ugalde, O. LUCAS Soil, the largest expandable soil dataset for Europe: A review. *European Journal of Soil Science* **69**, 140–153 (2018).

21. (ICRAF), W. A. & (ISRIC), I. S. R. A. I. C. ICRAF-ISRIC Soil VNIR Spectral Library. (2021) doi:10.34725/DVN/MFHA9C.

22. Hengl, T., Sanderman, J. & Parente, L. Open Soil Spectral Library (training data and calibration models). (2021) doi:10.5281/ZENODO.5759693.

23. Charman, D. J. *et al.* Climate-related changes in peatland carbon accumulation during the last millennium. *Biogeosciences* **10**, 929–944 (2013).

24. Gallego-Sala, A. V. *et al.* Latitudinal limits to the predicted increase of the peatland carbon sink with warming. *Nature Climate Change* **8**, 907–913 (2018).

25. Teickner, H. *et al.* Peatland mid-infrared database (1.0.0). (2025) doi:10.5281/zenodo.17092587.

26. Liu, H. & Lennartz, B. Hydraulic properties of peat soils along a bulk density gradient-A meta study. *Hydrological Processes* **33**, 101–114 (2019).

27. Hodgkins, S. B. *et al.* Tropical peatland carbon storage linked to global latitudinal trends in peat recalcitrance. *Nature Communications* **9**, 3640 (2018).

28. De la Cruz, F. B., Osborne, J. & Barlaz, M. A. Determination of sources of organic matter in solid waste by analysis of phenolic copper oxide oxidation products of lignin. *Journal of Environmental Engineering* **142**, 04015076 (2016).

29. Knierzinger, W. *et al.* Anthropogenic and climate signals in late-Holocene peat layers of an ombrotrophic bog in the Styrian Enns valley (Austrian Alps). *E&G Quaternary Science Journal* **69**, 121–137 (2020).

30. Knierzinger, W. (Bio)geochemical data Pürgschachen Moor. (2020).

31. Münchberger, W. Past and present carbon dynamics in contrasting South Patagonian bog ecosystems. (University Münster, Münster, 2019).

32. Münchberger, W., Knorr, K.-H., Blodau, C., Pancotto, V. A. & Kleinebecker, T. Zero to moderate methane emissions in a densely rooted, pristine Patagonian bog – biogeochemical controls as revealed from isotopic evidence. *Biogeosciences* **16**, 541–559 (2019).

33. Schuster, W. *et al.* Control of carbon and nitrogen accumulation by vegetation in pristine bogs of southern Patagonia. *Science of The Total Environment* **810**, 151293 (2022).

34. Drollinger, S., Kuzyakov, Y. & Glatzel, S. Effects of peat decomposition on δ^{13}C and δ^{15}N depth profiles of Alpine bogs. *CATENA* **178**, 1–10 (2019).

35. Drollinger, S., Knorr, K.-H., Knierzinger, W. & Glatzel, S. Peat decomposition proxies of Alpine bogs along a degradation gradient. *Geoderma* **369**, 114331 (2020).

36. Agethen, S. & Knorr, K.-H. *Juncus Effusus* mono-stands in restored cutover peat bogs – Analysis of litter quality, controls of anaerobic decomposition, and the risk of secondary carbon loss. *Soil Biology and Biochemistry* **117**, 139–152 (2018).

37. Kendall, R. A. Microbial and substrate decomposition factors in commercially extracted peatlands in Canada. (McGill University, Montréal, 2020).

38. Harris, L. I. *et al.* Permafrost thaw causes large carbon loss in boreal peatlands while changes to peat quality are limited. *Global Change Biology* gcb.16894 (2023) doi:10.1111/gcb.16894.

39. Harris, L. & Olefeldt, D. Permafrost thaw causes large carbon loss in boreal peatlands while changes to peat quality are limited. 10335101 bytes (2023) doi:10.5061/DRYAD.47D7WM3KK.

40. Pelletier, N. *et al.* Influence of Holocene permafrost aggradation and thaw on the paleoecology and carbon storage of a peatland complex in northwestern Canada. *The Holocene* **27**, 1391–1405 (2017).

41. Teickner, H., Gao, C. & Knorr, K.-H. Reproducible research compendium with R code and data for: 'Electrochemical properties of peat particulate organic matter on a global scale: Relation to peat chemistry and degree of decomposition'. (2021) doi:10.5281/zenodo.5792970.

42. Teickner, H., Gao, C. & Knorr, K.-H. Electrochemical properties of peat particulate organic matter on a global scale: Relation to peat chemistry and degree of decomposition. *Global Biogeochemical Cycles* **36**, e2021GB007160 (2022).

43. Heffernan, L. Peat carbon, δ^{14}C, macrofossil, and humification data from a thawing permafrost peatland in western Canada. (2019) doi:10.7939/DVN/MKM0ZE.

44. Heffernan, L., Estop-Aragonés, C., Knorr, K.-H., Talbot, J. & Olefeldt, D. Long-term impacts of permafrost thaw on carbon storage in peatlands: Deep losses offset by surficial accumulation. *Journal of Geophysical Research: Biogeosciences* **125**, (2020).

45. Broder, T., Blodau, C., Biester, H. & Knorr, K. H. Peat decomposition records in three pristine ombrotrophic bogs in southern Patagonia. *Biogeosciences* **9**, 1479–1491 (2012).

46. Anzenhofer, R. Biogeochemical characterization of peat profiles along a vegetation gradient in an ombrotrophic bog, Patagonia. (2014, unpublished).

47. Mathijssen, P. J. H., Gałka, M., Borken, W. & Knorr, K.-H. Plant communities control long term carbon accumulation and biogeochemical gradients in a Patagonian bog. *Science of The Total Environment* **684**, 670–681 (2019).

48. Wagner, S. Analysis of peat decomposition, element distribution patterns and element output of two peat bogs in the Thuringian Forest. (University Bayreuth, 2013).

49. Hömberg, A. Geochemische Charakterisierung von Mooren der Changbai Mountains. (Münster, Münster, 2014).

50. Berger, S., Gebauer, G., Blodau, C. & Knorr, K.-H. Peatlands in a eutrophic world – Assessing the state of a poor fen-bog transition in southern Ontario, Canada, after long term nutrient input and altered hydrological conditions. *Soil Biology and Biochemistry* **114**, 131–144 (2017).

51. Berger, S., Praetzel, L. S. E., Goebel, M., Blodau, C. & Knorr, K.-H. Differential response of carbon cycling to long-term nutrient input and altered hydrological conditions in a continental Canadian peatland. *Biogeosciences* **15**, 885–903 (2018).

52. Moore, T. R., Knorr, K.-H., Thompson, L., Roy, C. & Bubier, J. L. The effect of long-term fertilization on peat in an ombrotrophic bog. *Geoderma* **343**, 176–186 (2019).

53. Diaconu, A.-C. *et al.* A multi-proxy analysis of hydroclimate trends in an ombrotrophic bog over the last millennium in the Eastern Carpathians of Romania. *Palaeogeography, Palaeoclimatology, Palaeoecology* **538**, 109390 (2020).

54. Gałka, M. *et al.* Insight into the factors of mountain bog and forest development in the Schwarzwald Mts.: Implications for ecological restoration. *Ecological Indicators* **140**, 109039 (2022).

55. Gałka, M. *et al.* Relations of fire, palaeohydrology, vegetation succession, and carbon accumulation, as reconstructed from a mountain bog in the Harz Mountains (Germany) during the last 6200 years. *Geoderma* **424**, 115991 (2022).

56. Harris, L. I., Moore, T. R., Roulet, N. T. & Pinsonneault, A. J. Lichens: A limit to peat growth? *Journal of Ecology* **106**, 2301–2319 (2018).

57. Harris, L. I., Moore, T. R., Roulet, N. T. & Pinsonneault, A. J. Data from: Lichens: A limit to peat growth? (2019) doi:10.5061/dryad.s136dc8.

58. Boothroyd, I. M. *et al.* Sulfur constraints on the carbon cycle of a blanket bog peatland. *Journal of Geophysical Research: Biogeosciences* **126**, (2021).

59. Worrall, F. Sulphur constraints on the carbon cycle of a blanket bog peatland [dataset]. 3712 (2021) doi:10.15128/R2PK02C9794.

60. Reuter, H., Gensel, J., Elvert, M. & Zak, D. Infrared spectra (FTIR) of *Phragmites Australis* litter, initial and after anoxic decomposition in three wetland substrates. 10 data points (2019) doi:10.1594/PANGAEA.902069.

61. Reuter, H., Gensel, J., Elvert, M. & Zak, D. CuO lignin, and bulk decomposition data of a 75-day anoxic *Phragmites Australis* litter decomposition experiment in soil substrates from three northeast German wetlands. 1037 data points (2019) doi:10.1594/PANGAEA.902176.

62. Reuter, H., Gensel, J., Elvert, M. & Zak, D. Evidence for preferential protein depolymerization in wetland soils in response to external nitrogen availability provided by a novel FTIR routine. *Biogeosciences* **17**, 499–514 (2020).

63. Moore, T., Blodau, C., Turunen, J., Roulet, N. T. & Richard, P. J. H. Patterns of nitrogen and sulfur accumulation and retention in ombrotrophic bogs, eastern Canada. *Global Change Biology* **11**, 356–367 (2005).

64. Turunen, J., Roulet, N. T., Moore, T. R. & Richard, P. J. H. Nitrogen deposition and increased carbon accumulation in ombrotrophic peatlands in eastern Canada: N Deposition and Peat Accumulation. *Global Biogeochemical Cycles* **18**, (2004).

65. Leeper, T. J. tabulizer: Bindings for Tabula PDF table extractor library. (2018).

66. Jones, M. *et al.* *Ecological Metadata Language Version 2.2.0.* (2019) doi:10.5063/f11834t2.

67. Le Roux, G. & De Vleeschouwer, F. Preparation of peat samples for inorganic geochemistry used as palaeoenvironmental proxies. *Mires and Peat* **7**, (2010).

755 68. De Vleeschouwer, F., Chambers, F. M. & Swindles, G. T. Coring and sub-sampling of peatlands for palaeoenvironmental research. *Mires and Peat* **7**, 10 (2010).

69. Chambers, F. M., Beilman, D. W. & Yu, Z. Methods for determining peat humification and for quantifying peat bulk density, organic matter and carbon content for palaeostudies of climate and peatland carbon dynamics. *Mires and Peat* **10**, 1–10 (2011).

70. Courtney-Mustaphi, C. J. *et al.* Guidelines for reporting and archiving ^{210}Pb sediment chronologies to improve fidelity and extend data lifecycle. *Quaternary Geochronology* **52**, 77–87 (2019).

760

71. Khider, D. *et al.* PaCTS 1.0: A crowdsourced reporting standard for paleoclimate data. *Paleoceanography and Paleoclimatology* **34**, 1570–1596 (2019).

72. Mauquoy, D., Hughes, P. D. M. & van Geel, B. A protocol for plant macrofossil analysis of peat deposits. *Mires and Peat* **7**, 5 (2010).

765 73. Booth, R. K., Lamentowicz, M. & Charman, D. J. Preparation and analysis of testate amoebae in peatland palaeoenvironmental studies. *Mires and Peat* **7**, 7 (2010).

74. Beleites, C. & Sergo, V. hyperSpec: A package to handle hyperspectral data sets in R. (2021).

75. Baumann, P. simplerspec: Soil and plant spectroscopic model building and prediction. (2020).

770

76. Teickner, H. ir: Functions to handle and preprocess infrared spectra. (2022) doi:10.5281/ZENODO.6644806.

77. Teickner, H. pmird: R interface to the peatland mid-infrared database. (2025).

775 78. Teickner, H. & Knorr, K.-H. elco: Handling data on chemical element contents and isotope signatures. (2020).

79. Langel, R. & Dyckmans, J. A closer look into the nitrogen blank in elemental analyser/isotope ratio mass spectrometry measurements. *Rapid Communications in Mass Spectrometry* **31**, 2051–2055 (2017).

80. Pebesma, E., Mailund, T. & Hiebert, J. Measurement units in R. *R Journal* **8**, 486–

780 494 (2016).

81. Lasch, P. Spectral pre-processing for biomedical vibrational spectroscopy and microspectroscopic imaging. *Chemometrics and Intelligent Laboratory Systems* **117**, 100–114 (2012).

82. Wallace, W. E. & NIST Mass Spectrometry Data Center. Infrared Spectra. in *NIST Chemistry WebBook, NIST Standard Reference Database 69* (National Institute of Standards and Technology, Gaithersburg MD, 20899, 1997).

83. Linstrom, P. NIST Chemistry WebBook, NIST Standard Reference Database 69. (1997) doi:10.18434/T4D303.

84. Perez-Guaita, D., Kuligowski, J., Quintás, G., Garrigues, S. & de la Guardia, M. Atmospheric compensation in Fourier transform infrared (FT-IR) spectra of clinical samples. *Applied Spectroscopy* **67**, 1339–1342 (2013).

85. Stuart, B. H. *Infrared Spectroscopy: Fundamentals and Applications*. (John Wiley & Sons, Ltd, Chichester, UK, 2004). doi:10.1002/0470011149.

86. Parikh, S. J., Goyne, K. W., Margenot, A. J., Mukome, F. N. D. & Calderón, F. J. Soil chemical insights provided through vibrational spectroscopy. in *Advances in Agronomy* vol. 126 1–148 (Elsevier, 2014).

87. R Core Team. *R: A Language and Environment for Statistical Computing*. (R Foundation for Statistical Computing, Vienna, Austria, 2020).

88. Müller, K. *et al.* RMariaDB: Database interface and 'MariaDB' driver. (2021).

89. Csárdi, G. *et al.* remotes: R package installation from remote repositories, including 'GitHub'. (2021).

90. Schieferdecker, T., Müller, K. & Bergant, D. dm: Relational data models. (2022).

91. Teickner, H. & Hodgkins, S. irpeat 0.2.0: Functions to analyze mid-infrared spectra of peat samples. (2022) doi:10.5281/ZENODO.7262744.

92. Ucar, I., Pebesma, E. & Azcorra, A. Measurement errors in R. *R Journal* **10**, 549–557 (2018).

93. Teickner, H. Compendium of R code and data for "pmird: Peatland Mid Infrared Database 1.0.0". (2025).

Supporting information to: Peatland Mid-Infrared Database 1.0.0

Contents

Henning Teickner[1,2,*]
Svenja Agethen[1]
Sina Berger[3]
Rieke Inga Boelsen[4]
Werner Borken[5]
Luca Bragazza[6]
Tanja Broder[1]
Florentino B. De La Cruz[7]
Andrei-Cosmin Diaconu[8]
Nancy B. Dise[9]
Simon Drollinger[10]
Cristian Estop-Aragonés[1]
Mariusz Gałka[11]
Magalí Martí[12,13]
Stephan Glatzel[14]
Jessica Groß[1]
Lorna Harris[15]
Liam Heffernan[16]
Suzanne B. Hodgkins[17]
Annkathrin Hömberg-Grandjean[1]
Helga Hoppe[1]
Wolfgang Knierzinger[18]
Haojie Liu[19]
Paul J.H. Mathijssen[1,20]
Christopher Mollmann[1]
Wiebke Schuster[21]
Lisa Närtker[1]
David Olefeldt[15]
Verónica Pancotto[22,23]
Nicolas Pelletier[24]

Hendrik Reuter[25]
Bjorn Robroek[26,27]
Bosse Svensson[13]
Julie Talbot[28]
Lauren Thompson[29,30]
Fred Worrall[31]
Zhi-Guo Yu[32]
Klaus-Holger Knorr[1]

[1] Ecohydrology & Biogeochemistry Group, Institute of Landscape Ecology, University of Münster, Germany
[2] Spatiotemporal Modelling Lab, Institute for Geoinformatics, University of Münster, Germany
[3] Pädagogische Hochschule St.Gallen (PHSG), Notkerstrasse 27, 9000 St.Gallen, Switzerland
[4] Albert-Ludwigs-Universität Freiburg, Germany
[5] Soil Ecology, University of Bayreuth, Dr.-Hans-Frisch-Str. 1-3, 95448 Bayreuth, Germany
[6] Agroscope, Field-Crop Systems and Plant Nutrition, Nyon, Switzerland
[7] University of North Florida: Jacksonville, Florida, US
[8] Department of Geology, Babeş-Bolyai University, Kogalniceanu, 1, 400084, Cluj-Napoca, Romania
[9] UK Centre for Ecology & Hydrology Bush Estate, Penicuik, Edinburgh EH26 0QB, United Kingdom
[10] Bioclimatology, University of Göttingen, Göttingen, Germany
[11] University of Lodz, Faculty of Biology and Environmental Protection, Department of Biogeography, Paleoecology and Nature Conservation, Banacha 1/3, 90-237 Łodz, Poland
[12] Department of Biomedical and Clinical Sciences, Linköping University, Linköping, Sweden
[13] Department of Thematic Studies, Environmental Change, Linköping University, 58183 Linköping, Sweden
[14] Department of Geography and Regional Research, Geoecology, Faculty of Earth Sciences, Geography and Astronomy, University of Vienna, Vienna, Austria
[15] Department of Renewable Resources, University of Alberta, Edmonton, AB, T6G 2G7, Canada
[16] Department of Earth Sciences, Earth and Climate Cluster, Vrije Universiteit Amsterdam, Amsterdam, The Netherlands
[17] Department of Microbiology, The Ohio State University, Columbus, OH 43210, USA
[18] Federal Agency for Water Management, Institute for Land and Water Management Research, Petzenkirchen, 3252, Austria
[19] Faculty of Agricultural and Environmental Sciences, University of Rostock, Justus-von-Liebig-Weg 6, 18059 Rostock, Germany
[20] Climate Resilience, Wageningen Environmental Research, Wageningen University & Research, PO Box 47, NL-6700 AA, Wageningen, the Netherland
[21] Stiftung Naturschutz Schleswig-Holstein, Eschenbrook 4, 24113 Molfsee, Germany
[22] Centro Austral de Investigaciones Científicas (CADIC), Consejo Nacional de Investigaciones Científicas y Técnicas (CONICET), Ushuaia, Tierra del Fuego, Argentina

[23] Instituto de Ciencias Polares, Ambiente y Recursos Naturales (ICPA), Universidad Nacional de Tierra del Fuego (UNTDF), Ushuaia, Tierra del Fuego, Argentina
[24] Département de géographie, Université de Montréal, Canada
[25] Department of Ecohydrology and Biogeochemistry, Leibniz Institute of Freshwater Ecology and Inland Fisheries, Berlin, Germany
[26] Department of Ecology, Radboud Institute for Biological and Environmental Sciences, Faculty of Science, Radboud University Nijmegen, 6525 AJ Nijmegen, The Netherlands
[27] School of Biological Sciences, Faculty of Environmental and Life Sciences, University of Southampton, Southampton, SO17 1BJ, UK
[28] Département de Géographie, Université de Montréal, Campus MIL, 1375 Avenue Thérèse Lavoie-Roux, Montréal, Québec, H2V 0B3, Canada
[29] University of Alberta, Department of Renewable Resources, South Academic Building 348D, Edmonton, AB, T6G 2G7
[30] Hatfield Consultants, 1228 Kensington Rd NW Unit 305, Calgary, AB T2N 3P7
[31] Department of Earth Sciences, University of Durham, Durham, DH1 3LE, UK
[32] Ecohydrology Research Group, Dept. Hydrology & Water Resources, Nanjing University of Information Science and Technology, Ningliu Road. 219, 210000 Nanjing
* corresponding author(s): Henning Teickner (henning.teickner@uni-muenster.de)

Attributes in the 'pmird' database

Table S1: Definition of all attributes in the 'pmird' database.

Attribute name	Description	Unit
abbreviation	In table 'custom_units': A string representing an abbreviation for the custom unit.	-
abstract	A free text field with an abstract for the dataset.	-
acknowledgements	A free text field with acknowledgements for a dataset.	-
activity_137Cs	A numeric value representing the measured mean value of the ^{137}Cs activity of the sample [DPM g^{-1}] (DPM are disintegrations per minute).	g^{-1} min^{-1}
activity_137Cs_err	A numeric value representing the measurement error of the ^{137}Cs activity of the sample [DPM g^{-1}] (DPM are disintegrations per minute).	g^{-1} min^{-1}
activity_210Pb	A numeric value representing the measured mean value of the ^{210}Pb activity of the sample [Bq kg^{-1}].	Bq kg^{-1}
activity_210Pb_err	A numeric value representing the measurement error of the ^{210}Pb activity of the sample [Bq kg^{-1}].	Bq kg^{-1}
activity_226Ra	A numeric value representing the measured mean value of the ^{226}Ra activity of the sample [DPM g^{-1}] (DPM are disintegrations per minute).	g^{-1} min^{-1}

(Continued on Next Page...)

Table S1: *(continued)*

Attribute name	Description	Unit
activity_-226Ra_err	A numeric value representing the measurement error of the ^{226}Ra activity of the sample [DPM g^{-1}] (DPM are disintegrations per minute).	g^{-1} min^{-1}
Ag	A numeric value representing the silver mass content of the sample [mass-ppm].	μg g^{-1}
Ag_err	A numeric value representing the measurement error of the silver mass content value of the sample [mass-ppm].	μg g^{-1}
age_14C	A numeric value representing the mean value of the uncalibrated ^{14}C age of the sample [yr BP].	yr
age_14C_err	A numeric value representing the error of the uncalibrated ^{14}C age of the sample [yr].	yr
Al	A numeric value representing the aluminium mass content of the sample [mass-ppm].	μg g^{-1}
Al_err	A numeric value representing the measurement error of the aluminium mass content value of the sample [mass-ppm].	μg g^{-1}
apodisation_-function	A string representing the name of the apodisation function.	-
As	A numeric value representing the arsenic mass content of the sample [mass-ppm].	μg g^{-1}
As_err	A numeric value representing the measurement error of the arsenic mass content value of the sample [mass-ppm].	μg g^{-1}
attribute_-definition	A free text field with a textual description of the meaning of attributes in the pmird database.	-
attribute_name	A string describing the names of the attributes in all tables of the pmird database.	-
Ba	A numeric value representing the barium mass content of the sample [mass-ppm].	μg g^{-1}
Ba_err	A numeric value representing the measurement error of the barium mass content value of the sample [mass-ppm].	μg g^{-1}
background_-activity_-reached_210Pb	A logical value (TRUE or FALSE) indicating if the corresponding ^{210}Pb activity in the same row (activity_210Pb) represents (according to the interpretation of the person who dated the core) the supported (background) ^{210}Pb activity (TRUE) or not (FALSE).	-
beamsplitter_-name	A string representing the name of the beamsplitter.	-

(Continued on Next Page...)

Table S1: *(continued)*

Attribute name	Description	Unit
begin_date	The minimum value of "sampling_date" in table "samples" for a specific dataset.	-
bibtex	A string representing the bibtex code used for a literature reference throughout the pmird database.	-
bounds_-maximum	A numeric value representing the minimum possible value for a numeric attribute.	-
bounds_-minimum	A numeric value representing the maximum possible value for a numeric attribute.	-
Br	A numeric value representing the bromine mass content of the sample [mass-ppm].	μg g^{-1}
Br_err	A numeric value representing the measurement error of the bromine mass content value of the sample [mass-ppm].	μg g^{-1}
bulk_density	A numeric value representing the bulk density of the sample [g cm^{-3}].	g/cm^3
bulk_density_-210Pb	A numeric value representing the mass density of the subsample on which the ^{210}Pb activity of the sample was measured [g cm^{-3}].	g/cm^3
bulk_density_-210Pb_err	A numeric value representing the error of the mass density of the subsample on which the ^{210}Pb activity of the sample was measured [g cm^{-3}].	g/cm^3
bulk_density_-err	A numeric value representing the measurement error of the bulk density of the sample [g cm^{-3}].	g/cm^3
C	A numeric value representing the carbon mass content of the sample [mass-%].	g g^{-1}
C_err	A numeric value representing the measurement error of the carbon mass content value of the sample [mass-%].	g g^{-1}
Ca	A numeric value representing the calcium mass content of the sample [mass-ppm].	μg g^{-1}
Ca_err	A numeric value representing the measurement error of the calcium mass content value of the sample [mass-ppm].	μg g^{-1}
CaCO3	A numeric value representing the $CaCO_3$ mass content of the sample [µg g^{-1}]	μg g^{-1}
CaCO3_err	A numeric value representing the measurement error of the $CaCO_3$ mass content value of the sample [mass-ppm].	μg g^{-1}
change_date	A string with the date when a dataset was changed with the format YYYY-MM-DD.	-

(Continued on Next Page...)

Table S1: *(continued)*

Attribute name	Description	Unit
change_scope	In table 'maintenances': A string describing the scope to which the documented change was applied.	-
Cl	A numeric value representing the chlorine mass content of the sample [mass-ppm].	μg g^{-1}
Cl_err	A numeric value representing the measurement error of the chlorine mass content value of the sample [mass-ppm].	μg g^{-1}
comment	In table 'change_histories': A string with any comments on changes made to a dataset.	-
comments_-measurements	A free text field where you can enter all information related to the sample that is not covered by the remaining fields. For example you could provide information on potential contamination sources, issues with specific parameters, additional information to the sampling site, e.g. present vegetation, past vegetation, specific conditions during sampling, ...	-
comments_-samples	A free text field where you can enter all information related to the sample that is not covered by the remaining fields. For example you could provide information on potential contamination sources, issues with specific parameters, additional information to the sampling site, e.g. present vegetation, past vegetation, specific conditions during sampling, ...	-
common_name	A string representing a common taxon name.	-
core_label	A string representing a label for the peat core (if the sample was taken from a peat core). This can be a custom label.	-
counting_-method_210_-Pb	A string representing a description of the counting method used for measuring the ^{210}Pb activities (one of alpha, beta or gamma).	-
coverage_type	A string describing the type of a specific coverage (an entry in one of the tables "geographic_coverage", "temporal_coverage", or "taxonomic_coverage"). Must be one of "geographic_coverage", "temporal_coverage", "taxonomic_coverage".	-
Cr	A numeric value representing the chromium mass content of the sample [mass-ppm].	μg g^{-1}

(Continued on Next Page...)

Table S1: *(continued)*

Attribute name	Description	Unit
Cr_err	A numeric value representing the measurement error of the chromium mass content value of the sample [mass-ppm].	μg g^{-1}
Cu	A numeric value representing the copper mass content of the sample [mass-ppm].	μg g^{-1}
Cu_err	A numeric value representing the measurement error of the copper mass content value of the sample [mass-ppm].	μg g^{-1}
d13C	A numeric value representing the ^{13}C isotope signature of the sample in delta permil relative to the VPDB standard.	dimensionless
d13C_err	A numeric value representing the measurement error of the ^{13}C isotope signature of the sample in delta permil.	dimensionless
d15N	A numeric value representing the ^{15}N isotope signature of the sample in delta permil relative to air.	dimensionless
d15N_err	A numeric value representing the measurement error of the ^{15}N isotope signature of the sample in delta permil.	dimensionless
d18O	A numeric value representing the ^{18}O isotope signature of the sample in delta permil relative to VSMOW.	dimensionless
d18O_err	A numeric value representing the measurement error of the ^{18}O isotope signature of the sample in delta permil.	dimensionless
d2H	A numeric value representing the ^{2}H isotope signature of the sample in delta permil relative to VSMOW.	dimensionless
d2H_err	A numeric value representing the measurement error of the ^{2}H isotope signature of the sample in delta permil.	dimensionless
data_point_-number	A numeric value representing the number of data points in the spectrum.	-
description	A free text field. In table “custom_units”: A description of a custom unit. In table “maintenances“: A description of the maintenance of a dataset. In table “method_steps“: A description of a method step. In table ”quality_control”: A description of the quality control.	-
detector_-gain_factor	A numeric value representing the detection gain factor.	dimensionless
detector_name	A string representing the name of the detector.	-
dimension	A string representing the dimension of the unit.	-

(Continued on Next Page...)

Table S1: *(continued)*

Attribute name	Description	Unit
east_-bounding_-coordinate	A numeric value representing the east bounding values of a bonuding box around the sampling locations for a dataset (in the EPSG:3857 projection coordinate system — this is the system used by Google and is based on the WGS 84 reference system) [°E]. This is the minimum value in "sampling_longitude" from table "samples" for s specific dataset.	-
electron_-accepting_-capacity	A numeric value representing the electron accepting capacity (EAC) of the sample [μmol (g C)$^{-1}$].	μmol g^{-1}
electron_-accepting_-capacity_err	A numeric value representing the measurement error of the electron accepting capacity (EAC) of the sample [μmol (g C)$^{-1}$].	μmol g^{-1}
electron_-donating_-capacity	A numeric value representing the electron donating capacity (EDC) of the sample [μmol (g C)$^{-1}$].	μmol g^{-1}
electron_-donating_-capacity_err	A numeric value representing the measurement error of the electron donating capacity (EDC) of the sample [μmol (g C)$^{-1}$].	μmol g^{-1}
electronic_-mail_address	A string representing the email address for a person.	-
end_date	The maximum value of "sampling_date" in table "samples" for a specific dataset.	-
enthalpy_of_-formation	A numeric value representing the standard enthalpy of formation of the sample (using a molecular formular informed by element measurements of the sample) [kJ mol^{-1}].	kJ mol^{-1}
enthalpy_of_-formation_err	A numeric value representing the measurement error of the standard enthalpy of formation of the sample (using a molecular formular informed by element measurements of the sample) [kJ mol^{-1}].	kJ mol^{-1}
entropy_of_-formation	A numeric value representing the standard entropy of formation of the sample [J K^{-1} mol^{-1}].	J K^{-1} mol^{-1}
entropy_of_-formation_err	A numeric value representing the standard entropy of formation of the sample [J K^{-1} mol^{-1}].	J K^{-1} mol^{-1}
explanation	In table 'missing_value_codes': A string explaining what the corresponding missing value code means.	-
exponentiation_-factor	A numeric value representing the exponentiation factor used for file compression.	-

(Continued on Next Page...)

Table S1: *(continued)*

Attribute name	Description	Unit
Fe	A numeric value representing the iron mass content of the sample [mass-ppm].	μg g^{-1}
Fe_err	A numeric value representing the measurement error of the iron mass content value of the sample [mass-ppm].	μg g^{-1}
Fe2	A numeric value representing the Fe^{2+} mass content in the sample [mass-ppm]	μg g^{-1}
Fe2_err	A numeric value representing the measurement error of the Fe^{2+} mass content value of the sample [mass-ppm].	μg g^{-1}
Fe3	A numeric value representing the Fe^{3+} mass content in the sample [mass-ppm]	μg g^{-1}
Fe3_err	A numeric value representing the measurement error of the Fe^{3+} mass content value of the sample [mass-ppm].	μg g^{-1}
format_string	A string defining the format of a nominal variable.	-
general_-taxonomic_-coverage	In table 'taxonomic_coverage': A string describing the range of taxa addressed in the data set or collection.	-
geographic_-description	A free text field where the gepgraphic coverage for a dataset is described.	-
getting_started	A free text field where instructions to use the data are described.	-
Gibbs_-energy_of_-formation	A numeric value representing the standard Gibbs energy of formation of the sample [kJ mol^{-1}].	kJ mol^{-1}
Gibbs_-energy_of_-formation_err	A numeric value representing the measurement error of the standard Gibbs energy of formation of the sample [kJ mol^{-1}].	kJ mol^{-1}
given_name	A string rerpesenting the given name(s) of a person.	-
H	A numeric value representing the hydrogen mass content of the sample [mass-%].	g g^{-1}
H_err	A numeric value representing the measurement error of the hydrogen mass content value of the sample [mass-%].	g g^{-1}
heat_of_-combustion	A numeric value representing the heat of combustion of the sample (using a molecular formular informed by element measurements of the sample) [kJ mol^{-1}].	kJ mol^{-1}
heat_of_-combustion_err	A numeric value representing the measurement error of the heat of combustion of the sample (using a molecular formular informed by element measurements of the sample) [kJ mol^{-1}].	kJ mol^{-1}

(Continued on Next Page...)

Table S1: *(continued)*

Attribute name	Description	Unit
Hg	A numeric value representing the mercury mass content of the sample [mass-ppm].	μg g^{-1}
Hg_err	A numeric value representing the measurement error of the mercury mass content value of the sample [mass-ppm].	μg g^{-1}
holocellulose_-content	A numeric value representing the holocellulose content of the sample [mass-%].	g g^{-1}
holocellulose_-content_err	A numeric value representing measurement error of the holocellulose content of the sample [mass-%].	g g^{-1}
humidity_-absolute_-reference	A numeric value representing the absolute humidity during measurement of the reference (background).	g L^{-1}
humidity_-absolute_-sample	A numeric value representing the absolute humidity during measurement of the sample.	g L^{-1}
humidity_-relative_-reference	A numeric value representing the relative humidity during measurement of the reference (background).	kPa kPa^{-1}
humidity_-relative_sample	A numeric value representing the relative humidity during measurement of the sample.	kPa kPa^{-1}
hydraulic_-conductivity	A numeric value representing the saturated hydraulic conductivity (K_s) of the sample [cm h^{-1}].	cm h^{-1}
hydraulic_-conductivity_-err	A numeric value representing the error of the saturated hydraulic conductivity (K_s) of the sample [cm h^{-1}].	cm h^{-1}
id_attribute	An integer value representing an id for each attribute in the pmird database.	-
id_change_-history	An integer value representing an id for each entry in the table “change_histories“ in the pmird database.	-
id_citation	An integer value representing an id for each entry in the table “citations“ in the pmird database.	-
id_coverage	An integer value representing an id for each entry in the table “coverages“ in the pmird database.	-
id_dataset	A numeric id for the dataset (starting with 1 and increasing by 1; for one data contribution, this should be 1 for all samples and the appropriate id is assigned when the data are merged into the database).	-

(Continued on Next Page...)

Table S1: *(continued)*

Attribute name	Description	Unit
id_-geographic_-coverage	An integer value representing an id for each entry in the table “geographic_coverages“ in the pmird database.	-
id_instrument	An integer value representing an id for each entry in the table “instruments“ in the pmird database.	-
id_license	An integer value representing an id for each entry in the table “licenses“ in the pmird database.	-
id_-macrofossil_-type	A numeric id for the macrofossil type (starting with 1).	-
id_-maintenance	An integer value representing an id for each entry in the table “maintenances“ in the pmird database.	-
id_-measurement	A numeric id for measurements (starting with 1 and increasing by 1). This means that each measurement gets its own rows and measurements for different attributes are considered independent, i.e. multiple measurement ids for the same sample just count replicate measurements for any attribute. For attributes with less measurements than for a different attribute, just fill measurements starting from smaller id_measurement and leave the cells in the remaining rows empty.	-
id_-measurement_-scale	An integer value representing an id for each entry in the table “measurement_scales“ in the pmird database.	-
id_method	An integer value representing an id for each entry in the table “methods“ in the pmird database.	-
id_method_-step	An integer value representing an id for each entry in the table “mehod_steps“ in the pmird database.	-
id_missing_-value_code	An integer value representing an id for each entry in the table “missing_value_codes“ in the pmird database.	-
id_person	An integer value representing an id for each entry in the table “persons“ in the pmird database.	-
id_quality_-control	An integer value representing an id for each entry in the table “quality_controls“ in the pmird database.	-
id_sample	A numeric id for the sample (starting with 1 and increasing by 1).	-
id_site	A numeric id for the site where the sample was collected. This should be the corresponding value in the file site_info.csv.	-

(Continued on Next Page...)

Table S1: *(continued)*

Attribute name	Description	Unit
id_-taxonomic_-classification	An integer value representing an id for each entry in the table “taxonomic_classifications“ in the pmird database.	-
id_-taxonomic_-coverage	An integer value representing an id for each entry in the table “taxonomic_coverages“ in the pmird database.	-
id_temporal_-coverage	An integer value representing an id for each entry in the table “temporal_coverages“ in the pmird database.	-
id_unit	An integer value representing an id for each entry in the table “units“ in the pmird database.	-
identifier	In table ‘licenses‘: A string representing an identifier for the license.	-
In	A numeric value representing the indium mass content of the sample [mass-ppm].	μg g^{-1}
In_err	A numeric value representing the measurement error of the indium mass content value of the sample [mass-ppm].	μg g^{-1}
instrumentation	A string describing an instrument in the table “instruments” in the pmird database.	-
intellectual_-rights	A free text field describing any intellectual rights connected to a dataset.	-
introduction	A free text field providing an intriductory description to a dataset.	-
is_baseline_-corrected	A logical value indicating if a spectrum is already baseline corrected (TRUE) or not (FALSE).	-
K	A numeric value representing the potassium mass content of the sample [mass-ppm].	μg g^{-1}
K_err	A numeric value representing the measurement error of the potassium mass content value of the sample [mass-ppm].	μg g^{-1}
Klason_-lignin_content	A numeric value representing the Klason lignin content of the sample [mass-%].	g g^{-1}
Klason_-lignin_-content_err	A numeric value representing measurement error of the Klason lignin content of the sample [mass-%].	g g^{-1}
lab_code_14C	A string representing a code for the laboratory where the ^{14}C activities were measured (^{14}C ages were determined).	-
laboratory_-label_210Pb	A string representing a label (preferentially a code, similarly to lab_code_14C) for the laboratory where the ^{210}Pb activities were measured.	-

(Continued on Next Page...)

Table S1: *(continued)*

Attribute name	Description	Unit
language	A string representing a description for the language used in a dataset.	-
laser_-wavenumber	A numeric value representing the wavenumber of the laser.	-
license_name	A string representing the name of a license.	-
loss_on_-ignition	A numeric value representing the loss on ignition of the sample [mass-%].	g g^{-1}
loss_on_-ignition_err	A numeric value representing the measurement error of the loss on ignition value of the sample [mass-%].	g g^{-1}
macrofossil_-count	A numeric value representing a count for a specific macrofossil type (e.g. Carex seeds) divided by the volume of peat for which the macrofossil type was counted [cm^{-13}].	-
macrofossil_-presence	A logical value indicating if the respective macrofossil type was present in the peat sample (TRUE) or not (FALSE).	-
macrofossil_-size_lower	A numeric value representing the lower size bound for the macrofossil type (e.g. if only macrocharcoal particles larger than 1mm were considered) [mm].	mm
macrofossil_-size_upper	A numeric value representing the upper size bound for the macrofossil type (e.g. if wood fragments were classified by size) [mm].	mm
macrofossil_-taxon_organ	The same as attribute 'taxon_organ', but for macrofossils.	-
macrofossil_-type	A string representing the macrofossil type. This can be a custom value, such as 'vegetation', 'ash', 'charcoal', 'unidentifiable organic matter'.	-
macrofossil_-volume_-fraction	A numeric value representing the volumetric fraction of a specific macrofossil type in the peat sample [L L^{-1}]	L L^{-1}
macrofossil_-volume_-fraction_err	A numeric value representing measurement error for the volumetric fraction of a specific macrofossil type in the peat sample [L L^{-1}]	L L^{-1}
macroporosity	A numeric value representing the macroporosity of the sample [volume-%]. Since the term 'macroporosity' is ambiguous, the term should be defined in the description of the methods if values are available.	cm^3 cm^{-3}
macroporosity_-err	A numeric value representing the error of the macroporosityporosity of the sample [volume-%].	cm^3 cm^{-3}

(Continued on Next Page...)

Table S1: *(continued)*

Attribute name	Description	Unit
maintenance_-update_-frequency	In table 'maintenances': A string describing the frequency with which changes and additions are made to the dataset after the initial dataset is completed.	-
mass	A numeric value representing the mass of the sample [g]. This is the mass of the extracted sample and masses of subsets of the sample may differ (for example: A peat layer dried at 105°C may have a mass of 200 g. This is the value to be reported. After milling, 10 g may be used to measure the pH value (this value should not be reported here, but in the description of the methods or in column 'comments'.))	g
mass_210Pb	A numeric value representing the measured mass of the subsample on which the ^{210}Pb activity of the sample was measured [g].	g
mass_210Pb_-err	A numeric value representing the measurement error of the mass of the subsample on which the ^{210}Pb activity of the sample was measured [g].	g
mass_err	A numeric value representing the measurement error of the mass of the sample [g].	g
measurement_-date	A datetime representing the dat and time when the spectrum was measured.	-
measurement_-date_reference	A datetime representing the dat and time when the reference (background) spectrum was measured when a separate background spectrum is available in the file.	-
measurement_-device	A string representing the name of the measurement device.	-
measurement_-scale	In table 'measurement_scales': A string representing the measurmeent scale for a value.	-
Mg	A numeric value representing the magnesium mass content of the sample [mass-ppm].	μg g^{-1}
Mg_err	A numeric value representing the measurement error of the magnesium mass content value of the sample [mass-ppm].	μg g^{-1}
mir_co2_-contribution_-relative	A numeric value representing the relative carbon dioxide contribution to a mid infrared spectrum. This is the slope of an ordinary least squares regression model fitting a reference carbon dioxide spectrum to a specified range of the spectrum.	-

(Continued on Next Page...)

Table S1: *(continued)*

Attribute name	Description	Unit
mir_mode	A string representing the measurement mode in which the mid infrared spectra were measured. One of "absorbance_ftir", "atr_ftir", "dr_ftir".	-
mir_water_-vapor_-contribution_-relative	A numeric value representing the relative water vapor contribution to a mid infrared spectrum. This is the slope of an ordinary least squares regression model fitting a reference water vapor spectrum to a specified range of the spectrum.	-
mir_water_-vapor_-contribution_-relative_sd	A numeric value representing an uncertainty estimate for the relative water vapor contribution to a mid infrared spectrum. This is the standard deviation of the slope of an ordinary least squares regression model fitting a reference water vapor spectrum to a specified range of the spectrum.	-
mir_water_-vapor_-contribution_-relative_sd	A numeric value representing an uncertainty estimate for the relative water vapor contribution to a mid infrared spectrum. This is the standard deviation of the slope of an ordinary least squares regression model fitting a reference water vapor spectrum to a specified range of the spectrum.	-
mirs_file	A string representing the path to the file with the mid infrared spectrum for the sample. This is a relative path relative to the root of the database. This field should be left empty upon creating the project because the file path is added automatically when the data are included in the database.	-
missing_-value_code	A string representing a code for missing value in the tables "data", "samples", "macrofossils", and "mir_metadata" in the pmird database.	-
Mn	A numeric value representing the manganese mass content of the sample [mass-ppm].	μg g^{-1}
Mn_err	A numeric value representing the measurement error of the manganese mass content value of the sample [mass-ppm].	μg g^{-1}
multiplier_to_-si	A numeric value representing the value with which a given value with a certain measurement unit has to be multiplied in order to convert it to a related SI unit.	dimensionless
N	A numeric value representing the nitrogen mass content of the sample [mass-%].	g g^{-1}

(Continued on Next Page...)

Table S1: *(continued)*

Attribute name	Description	Unit
N_err	A numeric value representing the measurement error of the nitrogen mass content value of the sample [mass-%].	g g^{-1}
Na	A numeric value representing the sodium mass content of the sample [mass-ppm].	μg g^{-1}
Na_err	A numeric value representing the measurement error of the sodium mass content value of the sample [mass-ppm].	μg g^{-1}
Ni	A numeric value representing the nickel mass content of the sample [mass-ppm].	μg g^{-1}
Ni_err	A numeric value representing the measurement error of the nickel mass content value of the sample [mass-ppm].	μg g^{-1}
noise_level_-relative	A numeric value representing the relative noise level of a mid infrared spectrum.	-
north_-bounding_-coordinate	A numeric value representing the north bounding values of a bonuding box around the sampling locations for a dataset (in the EPSG:3857 projection coordinate system — this is the system used by Google and is based on the WGS 84 reference system) [°N]. This is the maximum value in “sampling_latitude” from table ”samples” for s specific dataset.	-
number_type	A string representing the number type of a numeric variable.	-
O	A numeric value representing the oxygen mass content of the sample [mass-%].	g g^{-1}
O_err	A numeric value representing the measurement error of the oxygen mass content value of the sample [mass-%].	g g^{-1}
old_value	In table ‘change_histories‘: A string describing the old dataset before the change in the current version.	-
online_url	In table ‘persons‘: A link to the website of a person.	-
P	A numeric value representing the phosphorous mass content of the sample [mass-ppm].	μg g^{-1}
P_err	A numeric value representing the measurement error of the phosphorous mass content value of the sample [mass-ppm].	μg g^{-1}
parent_si	A string representing the SI unit from which a certain derived unit is derived.	-
Pb	A numeric value representing the lead mass content of the sample [mass-ppm].	μg g^{-1}
Pb_err	A numeric value representing the measurement error of the lead mass content value of the sample [mass-ppm].	μg g^{-1}

(Continued on Next Page...)

Table S1: *(continued)*

Attribute name	Description	Unit
pH	A numeric value representing the pH value of the sample.	dimensionless
pH_err	A numeric value representing the measurement error of the pH value value of the sample.	dimensionless
phone	A string representing the phone number of a person.	-
porosity	A numeric value representing the porosity of the sample [volume-%].	$cm^3\ cm^{-3}$
porosity_err	A numeric value representing the error of the porosity of the sample [volume-%].	$cm^3\ cm^{-3}$
power	In table 'unit_types': An integer value. The power to which a dimension is raised.	-
pub_date	A string with the year when the dataset was originally published with the format YYYY.	-
purge_delay	A numeric value representing the duration of purge delay before a measurement in seconds.	s
purpose	A free text field dscribing the purpse for which the dataset was created.	-
Rb	A numeric value representing the rubidium mass content of the sample [mass-ppm].	$\mu g\ g^{-1}$
Rb_err	A numeric value representing the measurement error of the rubidium mass content value of the sample [mass-ppm].	$\mu g\ g^{-1}$
reference_-publication	A string in the bibtex format giving informatio on references which serve as references for data or publication where a certain dataset is described or used.	-
rep_no	An integer value representing the sample repetition number.	-
S	A numeric value representing the sulfur mass content of the sample [mass-ppm].	$\mu g\ g^{-1}$
S_err	A numeric value representing the measurement error of the sulfur mass content value of the sample [mass-ppm].	$\mu g\ g^{-1}$
salutation	A string representing the salutation used to address an individual.	-
sample_-depth_lower	A numeric value representing the depth of the lower boundary of a sample relative to the land surface (e.g. peat surface) [cm].	cm
sample_-depth_lower_-err	A numeric value representing the measurement error of the lower boundary of a sample [cm].	cm

(Continued on Next Page...)

Table S1: *(continued)*

Attribute name	Description	Unit
sample_-depth_upper	A numeric value representing the depth of the upper boundary of a sample relative to the land surface (e.g. peat surface) [cm].	cm
sample_-depth_upper_-err	A numeric value representing the measurement error of the upper boundary of a sample [cm].	cm
sample_label	A string representing a label for each sample.	-
sample_-microhabitat	A string describing the microhabitat where the sample was collected. For peat, this should be one of 'hummock', 'hollow', 'lawn', 'pond'. In other cases, a custom value can be used.	-
sample_-treatment	A string with an description of an experimental tratment if this was applied. By default, this should be 'control', indicating that there was no manipulation. If there was any experimental manipulation, this can be abbreviated by a label (e.g. by a treatment level) that is defined in the textual description of the project (in the file 'description.docx').	-
sample_type	A string describing the type of the sample. Must be one of 'peat', 'dom', 'vegetation', 'litter'.	-
sample_type2	A string describing the type of the sample. Here you can provide individual (own) categories which may provide more details than the column sample_type.	-
sampling_-altitude	A numeric value representing the altitude of the exact sampling position [m above sea level].	m
sampling_-altitude_err	A numeric value representing the measurement error of the altitude of the exact sampling position [m above sea level].	m
sampling_date	A string with the date when the sample was collected (in the field) with the format YYYY-MM-DD.	-
sampling_-description	A free text field where the collection of samples is described (including experimental or sampling design).	-
sampling_-latitude	A numeric value representing the latitude coordinates of the exact sampling position (in the EPSG:3857 projection coordinate system — this is the system used by Google and is based on the WGS 84 reference system) [°N].	-

(Continued on Next Page...)

Table S1: *(continued)*

Attribute name	Description	Unit
sampling_-latitude_err	A numeric value representing the measurement error of the latitude coordinates of the exact sampling position (in the EPSG:3857 projection coordinate system — this is the system used by Google and is based on the WGS 84 reference system) [°N].	-
sampling_-longitude	A numeric value representing the longitude coordinates of the exact sampling position (in the EPSG:3857 projection coordinate system — this is the system used by Google and is based on the WGS 84 reference system) [°W].	-
sampling_-longitude_err	A numeric value representing the measurement error of the longitude coordinates of the exact sampling position (in the EPSG:3857 projection coordinate system — this is the system used by Google and is based on the WGS 84 reference system) [°W].	-
Sb	A numeric value representing the antimony mass content of the sample [mass-ppm].	μg g^{-1}
Sb_err	A numeric value representing the measurement error of the antimony mass content value of the sample [mass-ppm].	μg g^{-1}
scan_number	An integer value representing the number of scans.	-
scan_speed	A numeric value representing the scan speed.	kHz
Si	A numeric value representing the silicium mass content of the sample [mass-ppm].	μg g^{-1}
Si_err	A numeric value representing the measurement error of the silicium mass content value of the sample [mass-ppm].	μg g^{-1}
Sn	A numeric value representing the tin mass content of the sample [mass-ppm].	μg g^{-1}
Sn_err	A numeric value representing the measurement error of the tin mass content value of the sample [mass-ppm].	μg g^{-1}
source_name	A string representing the name of the infrared radiation source.	-

(Continued on Next Page...)

Table S1: *(continued)*

Attribute name	Description	Unit
south_-bounding_-coordinate	A numeric value representing the south bounding values of a bonuding box around the sampling locations for a dataset (in the EPSG:3857 projection coordinate system — this is the system used by Google and is based on the WGS 84 reference system) [°N]. This is the minimum value in "sampling_latitude" from table "samples" for s specific dataset.	-
Sr	A numeric value representing the strontium mass content of the sample [mass-ppm].	μg g^{-1}
Sr_err	A numeric value representing the measurement error of the strontium mass content value of the sample [mass-ppm].	μg g^{-1}
standard_unit	A logical value indicating whether the unit is a standard unit of the Ecological Metadata Language or not.	-
sur_name	A string representing the sur name of a person.	-
taxon_organ	A string describing the organ of a taxon the sample represents (if the sample represents a taxon). For example, if the sample is Carex lasiocarpa, this could be 'shoot', or 'root', or 'leaves'.	-
taxon_rank_-name	A string describing the taxon rank the value in column taxon_rank_value represents (if the sample can be assigned to a specific taxon). For exampe, if the value in column taxon_rank_value is a species name, then you should enter 'species' here, or if the value in column taxon_rank_value is a genus name, then you should enter 'genus' here.	-
taxon_rank_-value	A string describing the taxon rank value of the sample (if the sample can be assigned to a taxon). For example, if the sample is a distinct species, enter the scientific species name here, or if the sample can be assigned to a genus, enter the scientific genus name here.	-
temperature_-scanner_-reference	A numeric value representing the temperature of the scanner during the measurement of the reference (background).	K
temperature_-scanner_-sample	A numeric value representing the temperature of the scanner during the measurement of the sample.	K
text_domain_-definition	A string representing the text domain for a string.	-

(Continued on Next Page...)

Table S1: *(continued)*

Attribute name	Description	Unit
Ti	A numeric value representing the titanium mass content of the sample [mass-ppm].	μg g^{-1}
Ti_err	A numeric value representing the measurement error of the titanium mass content value of the sample [mass-ppm].	μg g^{-1}
title	A free text field with the title for a dataset.	-
udunits_unit	A string representing a measurement unit in the udunits format.	-
unit_type	A string representing the type of a unit.	-
url	In table 'licenses': A string representing an url to a website with information on the license.	-
user_id	In table 'persons': A string representing an identifier that links this party to a directory of individuals.	-
volume	A numeric value representing the volume of the sample [cm^3].	cm^3
volume_210Pb	A numeric value representing the measured volume of the subsample on which the ^{210}Pb activity of the sample was measured [cm^3].	cm^3
volume_-210Pb_err	A numeric value representing the error of the volume of the subsample on which the ^{210}Pb activity of the sample was measured [cm^3].	cm^3
volume_err	A numeric value representing the measurement error of the volume of the sample [cm^3].	cm^3
water_content	A numeric value representing the water mass content of the sample as mass of water divided by the mass of the wet sample [g g^{-1}]	g g^{-1}
water_-content_err	A numeric value representing the measurement error of the water mass content value of the sample [g g^{-1}].	g g^{-1}
west_-bounding_-coordinate	A numeric value representing the west bounding values of a bonuding box around the sampling locations for a dataset (in the EPSG:3857 projection coordinate system — this is the system used by Google and is based on the WGS 84 reference system) [°E]. This is the maximum value in "sampling_longitude" from table "samples" for s specific dataset.	-
x_variable_-max	A numeric value representing the maximum x variable value of each spectrum.	cm^{-1}
x_variable_-min	A numeric value representing the minimum x variable value of each spectrum.	cm^{-1}

(Continued on Next Page...)

Table S1: *(continued)*

Attribute name	Description	Unit
x_variable_-type	A string representing the type of the x variable.	-
y_variable_-type	A string representing the type of the y variable.	-
year_137Cs	A numeric value representing the age that was assigned to the sample based on the ^{137}Cs activity inventory [yr AD] (e.g. by relating it to the date of the Chernobyl accident).	yr
zero_filling_-factor	An integer value representing the zero filling factor.	-
Zn	A numeric value representing the zinc mass content of the sample [mass-ppm].	μg g^{-1}
Zn_err	A numeric value representing the measurement error of the zinc mass content value of the sample [mass-ppm].	μg g^{-1}
Zr	A numeric value representing the zirconium mass content of the sample [mass-ppm].	μg g^{-1}
Zr_err	A numeric value representing the measurement error of the zirconium mass content value of the sample [mass-ppm].	μg g^{-1}

Example of the method description for dataset 8

Table S2: Method and method steps description for dataset 8 in the 'pmird' database.

id_method	id_method_step	description
40	56	Two coring locations were chosen to contrast on the one hand former bog parts used for peat extraction, with 1 m old grown peat left, which are restored by ditch-blocking and flooding since the middle of the 1970's , and where only young birches grow (max. height 4 m) (coring location 1: cores 1 to 2), and on the other hand old peat bodies not used for peat extraction, but strongly drained and overgrown by taller trees with few actively growing *Sphagna* (coring location 2: cores 3 to 5). sampling_longitude and sampling_latitude values refer to the coring locations and the different peat cores were taken in a distance of 20 cm to this location. At each coring location, two to three cores were taken, where a peat core is a set of peat samples taken at the same position. At location 1, the upper 30 cm had a too small bulk density to be sampled with a peat corer. Instead, a grab sample with the help of a stainless steel knife was taken (core 1, segment 1). In the resulting hole, segment 2 of core 1 was taken with a Russian peat corer (50 cm length). 20 cm next to the location where core 1 was taken, a second core was taken with the Russian peat corer after removing the top 30 cm peat. Core 2 was used for measurement of element contents and isotope signatures, bulk density, water content, and mid infrare spectra. Core 1 was used exclusively for pH measurements, except for segment 1 which was also used for laboratory analyses.

(Continued on Next Page...)

Table S2: *(continued)*

id_method	id_method_step	description
		At location 2, a 50 cm peat core for pH measurements was taken with the Russian peat corer (core 3). A second core (core 4) consisting of 5 segments with a total length of 250 cm was taken at a distance of 20 cm. During this, the tip of the corer might have compressed subsequent peat layers. This peat core was cut into 2 cm sections (upper 50 cm) and 5 cm sections (below 50 cm). This core was used to measure element contents and isotope signatures, bulk density, water content, and mid infrare spectra. Due to low bulk densities of the uppermost layers of core 4 (consisting mainly of fallen leaves from trees and few *Sphagna*), the material would not have been sufficient for all laboratory analyses. Therefore 20 cm next to the coring location of core 4, we took a grab sample by cutting a 6 cm · 6 cm block of peat which was separated into 2 cm layers using a stainless steel knife (core 5). Peat cores were transported horizontally, placed onto two boxes and cut by hand with a stainless steel knife using a folding rule as depth reference. Samples to be used for laboratory analyses were placed into Whirl-Paks which were placed into transportable cooling boxes. The samples were freezed after 6 (core 2, upper 30 cm of core 1) and 4 (core 4 and 5) hours.
40	1	Freeze drying
40	57	Freeze-dried samples were milled in a vibrating cup mill with tungsten carbide cups and balls.
40	58	Freeze-dried and milled samples were analyzed with an elemental analyzer coupled to an isotope ratio mass spectometer to measure C and C contents and stable isotope signatures against VPDB and air, respectively. For this, samples are catalytically combusted and contents are determined via gas chromatography. Isotope signatures and element contents were corrected with the R package elco Teickner and Knorr (2020) using standards measured during the same runs as the samples. Duplicate measurements are remeasurements due to signal loss during the measurements.

(Continued on Next Page...)

Table S2: *(continued)*

id_method	id_method_step	description
40	59	For each sample, 2 mg freeze-dried and milled sample material were mixed with 200 mg KBr (FTIR grade, Sigma Aldrich, St. Louis, MO, USA) using an agate mortar and pestle and pressed to a pellet. MIR spectra were measured with an FTIR spectrometer in absorbance mode by averaging 32 scans. The spectra were background corrected with a pure KBr pellet.
40	60	Water content was computed by dividing the difference between the wet and dry mass by the wet mass of each sample. Sample masses were measured with packaging (Whirl-Paks) and sample masses without packaging were computed by subtracting the mass of two empty, clean Whirl-Paks, each measured five times. Measurement errors were estimated for the Whirl-Pak masses as the sample standard deviation of the replicate measurements. The same errors were assumed for the other weighed masses. Errors were propagated during computations using the R package quantities.
40	61	Bulk densities were computed by dividing the dry mass by the volume for each sample. Sample masses were measured with packaging (Whirl-Paks) and sample masses without packaging were computed by subtracting the mass of two empty, clean Whirl-Paks, each measured five times. Measurement errors were estimated for the whirl pack masses as the sample standard deviation of the replicate measurements. The same errors were assumed for the other weighed masses. Errors were propagated during computations using the R package quantities. Volumes were computed from the dimensions of the samples in the field (not considering depth errors during peat core slicing or dimension errors for grab samples). Volume errors were not considered during error propagation.
40	62	pH values were measured in the field according to method 4C1a1a4 of the USDA Kellog Soil Survey Laboratory Methods Manual (version 5.0). For this, 2.5 mL wet sample material was mixed with 4 mL 0.015 mol L^{-1} $CaCl_2$, stirred by hand, and left unmoved for one hour. After stirring again, the pH value was measured in the supernatant.